Evolved phenological cueing strategies show variable responses to climate change

Collin B. Edwards[1] and Louie H. Yang[2]

[1]Department of Ecology and Evolutionary Biology, Cornell University, E451 Corson Hall, Ithaca, NY 14853 USA

[2]Department of Entomology and Nematology, University of California, Davis, CA 95616 USA

Several studies have documented a global pattern of phenological advancement across multiple taxa that is consistent with ongoing climate change[1–3]. However, the magnitude of these phenological shifts is highly variable across taxa and locations[2–4]. This variability of phenological responses disrupts species interactions under climate change[5–9], but has been difficult to explain mechanistically[10–13]. To understand how climate change could evoke such variable responses in different groups of organisms, we constructed a model for the evolution of phenological cueing strategies using historic climate data from 78 locations in North America and Hawaii. Here we show how phenological cueing strategies can evolve in predictable ways, but still express highly variable responses to climate change. Across locations, organisms in our model evolved diverse strategies that reflected geographic differences in the reliability of different environmental cues for predicting future conditions. Within locations, a wide range of evolved strategies showed similar emergence phenotypes under historical conditions. However, these same strategies revealed previously hidden and variable responses under novel climatic conditions, with strong fitness consequences. These cryptic differences in cueing strategies evolved under historical conditions because epistasis and non-additive genotype × environment interactions among years resulted in weak selection gradients across an extensive region of trait space. These findings show how the evolution of integrated phenological cueing strategies can explain observed variation in phenological shifts and unexpected responses to climate change.

Recent years have seen increasing interest in the study of phenological shifts. While organisms around the world have generally shown a "global coherent fingerprint" of advancing phenology with climate change[1–3], several studies also point to substantial unexplained variation in phenological shifts[2–4]. This variation in responses to climate change is an important factor driving phenological mismatch and the disruption of species interactions[8,9]. It has become increasingly clear that understanding how organisms integrate multiple environmental cues will be necessary to explain and predict phenological shifts[10–13].

In order to examine the causes of variation in phenological shifts, we developed a model that simulates how different environmental histories shape the evolution of phenological cueing strategies. We hypothesized that organisms experiencing different environmental histories would evolve different phenological strategies, caused by consistent differences in the reliability of predictive information provided by different kinds of environmental cues. We further hypothesized that these variable strategies create variation in phenological responses to climate change.

Our model simulates the evolution of a generalized organism in a simplified environment defined by daily maximum temperature, total daily precipitation, and day of the year (hereafter, temperature, precipitation and day). These environments are drawn from historic climatic records representing an average of 98 years from each of 78 locations in North America and Hawaii. In our model, these real-world environmental data provide cues to anticipate future environmental conditions each year, and also determine the fitness of individuals in the population (Extended Data Fig. 1). The environmental cues (E) on each day are cumulative annual daily maximum temperature (γ_{temp}), cumulative annual daily precipitation (γ_{precip}), and day of year (γ_{day},):

$$E = [\gamma_{temp}, \gamma_{precip}, \gamma_{day}] \qquad (1)$$

The use of cumulative annual temperature and precipitation is based on the assumption that organisms are aware of and can be influenced by past environmental conditions, consistent with degree-day models of development and phenology. Each individual has a genotype (G) defined by three traits (τ), which reflect its sensitivity to the three environmental cues:

$$G = [\tau_{temp}, \tau_{precip}, \tau_{day}] \qquad (2)$$

Each day of the simulation, each individual combines its cues and genotype into a weighted sum, which represents the emergence signal (S):

$$S = \frac{\gamma_{temp}}{\tau_{temp}} + \frac{\gamma_{precip}}{\tau_{precip}} + \frac{\gamma_{day}}{\tau_{day}} \qquad (3)$$

When this signal crosses the threshold S≥1, the organism makes an irreversible decision to emerge. Its fitness is then dependent on daily temperature and moisture conditions over a fixed window, beginning one day after the threshold is crossed. We defined fitness as a function of daily temperature and moisture using a multivariate skew-normal distribution with optimal temperature and moisture values set to the 90th percentile of all values observed in a given location. This assumes that fitness is a fixed, asymmetric function of environmental conditions and that physiological performance is adapted to past local conditions. For each location, we ran 60 simulations with the same parameters. Each simulation included 1000 randomly resampled years of climatic data and a population of 500 individuals whose initial genotypes were drawn from a broad uniform random distribution (Extended Data Fig. 2).

The results of this model suggest two key findings. First, the mean evolved strategies of each location in our model are spatially autocorrelated, indicating that similar strategies evolved in locations that experienced similar climates, while individuals from different climates consistently evolved different strategies (Fig. 1, Fig. 2, Extended Data Fig. 3 and Extended Data Fig. 4). These evolved differences reflect geographic differences in the relative reliability of temperature, precipitation and day cues for predicting future fitness outcomes. This finding was qualitatively robust across model variants that used different cues, fitness functions, and emergence durations (Extended Data Fig. 5). We evaluated several climatic and location-based variables in order to explain the pattern of evolved cueing strategies, but most showed small or counterintuitive effects (Extended Data Fig. 6). In general, these evolved strategies did not conform to predictions based on simple assumptions about latitude, climatic variability, predictability or seasonality[14,15]; instead, they illustrated the complexity of the location-specific climatic regimes and fitness landscapes that affect organisms in this model. Selection favored cues based on their ability to predict future environmental conditions – both the ability to consistently trigger emergence ahead of favorable conditions, and the ability to avoid triggering emergence ahead of

unfavorable conditions. Although the simplified environmental data in our model showed unexpected complexity, the spatial autocorrelation of evolved strategies in our model suggests that information constrains the evolution of phenological cueing strategies in predictable ways.

The second key finding of this model is that repeated simulations from the same location produced diverse strategies that expressed similar phenotypes under historical conditions (Figs. 2 and 3, Extended Data Fig. 3), but showed strong phenotypic and fitness differences under simulated climate change (Fig. 4, Extended Data Fig. 7). This finding was an unanticipated consequence of cue integration, which allows a wide range of strategies to be almost equally effective under the same environmental conditions. This pattern emerges in our model because the function combining environmental conditions and traits is non-injective: multiple combinations of traits can yield the same expressed phenotype. In our model, multiple cues are combined to yield a single emergence signal; in this context, epistatic interactions between traits mean that increased sensitivity to one cue can compensate for reduced sensitivity to another. Moreover, the expressed phenotype results from a non-additive genotype × environment interaction which allows genotypes to show different reaction norms across years[16], driven by the complex structure of real-world climate data. On average, genotype x environment interactions explained 29% of observed fitness variation across all locations (Extended Data Fig. 8). As a result, the phenotypic and fitness differences between evolved genotypes are inconsistent from year to year in a way that reduces the long-term mean fitness differences between genotypes (Extended Data Fig. 9). The outcomes of these processes are weak selection gradients across a wide range of trait space (Extended Data Fig. 10). The resulting diversity of phenological cueing strategies could contribute to observed variation in phenological responses to climate change[2,3,17] and the evolution of cryptic genetic variation[18,19].

Climate change had a strong effect on both phenotypes and fitness in most locations (Fig. 4, Extended Data Fig. 7). We modeled two simple climate change scenarios. In the first ("shift") scenario, we advanced both temperature and precipitation regimes by 5 d. In the second ("warming") scenario, we increased all daily maximum temperatures by 3°C. With each changed climate regime, the mean genotypes that evolved under historical conditions in 30 simulations were evaluated against all available years. In both scenarios, populations advanced their phenology and generally showed reduced fitness (Fig. 4). These effects were non-random; for example, organisms in the shift scenario that relied more on day cues were less likely to advance their emergence timing on pace with the changed climate ($\chi^2(1)=466.7$, $p<0.00001$), and generally showed negative fitness consequences relative to individuals that favored temperature or precipitation cues ($\chi^2(1)=11.1$, $p=0.0009$, Fig. 4). This result is consistent with expectations about the costs of relying on invariant day-of-year cues under a climate change scenario[20,21], and the potential for adaptive plasticity in response to changing climates. By comparison, under the warming scenario, organisms with greater reliance on day cues also showed reduced phenological advancement ($\chi^2(1)=35.5$, $p<0.00001$), but generally showed higher fitness than organisms that were more reliant on climatic cues ($\chi^2(1)=9.0$, $p=0.0026$). This unexpected result occurs because the warming scenario broke the historic correlation structure between temperature- and precipitation-based factors in most climates, causing many strategies to demonstrate maladaptive plasticity in a novel climate[22,23].

The key prediction of this model is that evolved phenological cueing strategies will show hidden variation in their responses to climate change. In our model, environmental history shaped the evolution of phenological cueing strategies in ways that reflected local differences in environmental conditions.

However, instead of favoring a single climatically-determined optimum strategy in each location, selection produced substantial variation in the ways individuals combined multiple cues to determine their emergence phenology. Importantly, the fundamental mechanisms driving this finding will emerge from any reasonable model of cue integration where multiple cues are combined to inform phenological decisions. This underlying principle likely contributes to the observed variability of phenological responses to novel climates around the world, and challenges our ability to predict phenological responses and fitness consequences under climate change. Developing a stronger understanding of phenological cueing mechanisms may improve our ability to understand and predict the ecological effects of climate change.

Methods

Environmental data

All available years of daily maximum temperature (degrees Celsius) and daily precipitation (mm rainfall equivalent) data were obtained from the NOAA Climate Data Online portal[24] for 82 locations in North America and Hawaii. Years with <325 daily temperature and precipitation observations were excluded from further analysis, and four locations with <50 years of data remaining were also excluded. For each of the remaining 78 locations, the interquartile range (IQR) was calculated as the difference between first quartile (Q_1) and third quartile (Q_3) observations. Temperature observations less than (Q_1-4*IQR) and greater than (Q_3+4*IQR) were identified as extreme outliers likely resulting from measurement error, and were excluded; such outliers were a small proportion (0.0012%) of the overall dataset. Missing observations in the remaining dataset (less than 1% of observations) were imputed using an expectation-maximization with bootstrapping (EMB) algorithm. Imputed values for temperature and precipitation were bounded by the observed minimum and maximum values of each location, and informed by priors based on the means and standard deviations of each location. This procedure imputed a complete dataset of daily maximum temperatures and daily precipitation for each location, with an average duration of 98 years (SD = 18.9 years).

Organisms used cumulative temperature and precipitation as climatic cues, and their fitness was affected by daily temperature and moisture during their emergence period. Temperature for each location was shifted so that the minimum transformed temperature for that location was zero. This meant that cue values were always non-negative. Environmental moisture (*m*) was calculated based on daily precipitation totals (*p*) in the dataset using a formula that includes a proportional retention constant (α, set to 0.8) to represent the partial retention of moisture over time, as well as the input of new precipitation each day (p). Changing the retention constant did not qualitatively change the model.

$$m_t = m_{t-1}\alpha + p_t \qquad (4)$$

Day of the year was represented as an integer value reflecting the number of days since January 1 of each year inclusive. The 366th day was truncated from leap years in the dataset. Day of year provides a proxy for a consistent and non-climatic environmental cue akin to photoperiod, implicitly assuming physiological mechanisms in each organism that are able to infer the day of the year from photoperiodic dynamics with equal accuracy across all locations. This simplifying assumption is supported by studies showing that although the amplitude photoperiodic changes is larger at higher latitudes, tropical species are able to detect the extremely small changes in photoperiod that occur near the equator[25,26]. This assumption also allows us to infer the relative information content of day as a cue across multiple

locations, separate from the effect of increasing photoperiodic amplitude at higher latitude. In examining spatial variation in the evolution of phenological strategies, day of year conservatively assumes that the phenological information available to organisms is unaffected by latitude. Using cumulative photoperiod produced qualitatively similar results (e.g., Extended Data Figure 5).

Emergence signal

Organisms in our model accrue fitness for 10 days after the emergence signal exceeds 1. To facilitate interpretation, this emergence signal model uses linear coefficients equal to the inverse of the trait value, so that genotypic traits are represented in same units as the cue itself, and trait values indicate the critical cue value that would trigger emergence in the hypothetical absence of other cues. Thus, large trait values correspond to low sensitivity and small trait values correspond to high sensitivity to the corresponding cue.

Fitness and reproduction

Individuals that emerge reproduce at a rate proportional to the cumulative fitness they accrue over their lifespan. The fitness gained on any given day is the product of two skew-normal function outputs – one based on temperature, the other on moisture. The thermal performance curves of ectotherms are generally asymmetrical, with a sharp decline above their optimal temperature and a more gradual decline below it[27,28]. For simplicity, we used the same skew normal functional form (with a skew parameter of -10) for both temperature and moisture. This function was parameterized separately for each location for both temperature and moisture, such that the peak for each occurred at the 90th percentile of temperature and of moisture of all daily observations for a given location, and the function had a value that was 10 percent of the peak when the cue was at the 10th percentile of all daily observations. This parameterization assumes that organisms are physiologically adapted to the prevailing conditions at each location, with an expected 10% of temperature and moisture values exceeding the optimal values. To evaluate the robustness of observed results, we tested this model at a range of alternative fitness parameterizations with qualitatively identical results (see below). Because the skew normal function does not have a simple mathematical relationship between its parameters and the location of the peak, we fit parameter values by minimizing the sum of squared errors. After both skew normal functions were parameterized, we calculated the daily fitness payoff for each day in each year of each climate as the product of the two skew normal function outputs. The fitness of each emerged individual (W_i) was calculated as the sum of daily fitness payoffs over its lifespan. Organisms that did not emerge by the end of the year received zero fitness. Individuals reproduced asexually with mutation (see below), with population size held constant at 500 individuals and expected realized fitness of each individual proportional to its calculated relative fitness. Reproduction was implemented as a lottery model to allow for demographic stochasticity. For each evolved strategy in the final generation, we calculated its geometric mean fitness across all years.

Heritability and mutation

Offspring genotypes reflected the trait values of their parent, modified by mutation. We modeled mutation by adding random numbers drawn from a normal distribution with mean 0 and a small standard deviation to the traits of all individuals in each generation. We set the standard deviation of mutation to be 0.5 percent of the overall cue range in order to produce mutation distributions with the

same expected effect size in each location. In the case of the day cue, we used 360 as the maximum, leading to a standard deviation of 1.8 for mutation rate of the day trait in all locations.

Initialization and execution

For each simulation, each individual in the initial generation was assigned uniform random trait values between 0 and 4*(the maximum cue value in that location, or 360 in the case of the day cue). This results in an initial population of individuals with emergence phenotypes ranging between emerging on day 1 and never emerging. Each simulation run experienced 1000 years of environmental conditions drawn by year with replacement from the set of available environmental data for that location (e.g., Extended Data Figure 2).

Assessing realized relative cue use

We define the "trait effect" (T) as a metric of proportional cue use in order to assess the relative degree to which an organism's emergence decision was affected by each environmental cue. This metric quantifies each organism's realized reliance on different cues represented by the proportion of the emergence signal that is contributed by each $\frac{\gamma}{\tau}$ term on the day emergence is triggered. This metric allows the relative contribution of each cue type to be compared across locations. The trait effect metric also allows realized relative cue use to be analyzed as a dataset of mathematical compositions, and thus plotted on ternary plots. Because of the discontinuous nature of daily cues, individuals might have an S > 1 when they emerged; we rescaled the trait effect values for each individual so that they sum to 1. For each individual in the final population at the end of each simulation, we calculated the Aitchison compositional mean[3] of the trait effects that would have been realized for each year of actual climate data used. This compositional mean represents the expected relative cue use of that genotype in the historic environment.

Sensitivity analyses

We conducted sensitivity analyses using a range of values for lifespan, lag, moisture decay parameter α, and normal and skew-normal fitness distributions using different optimal temperature and moisture values. All parameters and distributions yielded qualitatively identical results, and we present a representative set of model parameters. We also tested additional climatic cues, including daily temperature and moisture, cumulative photoperiod, and quadratic formulations of temperature, moisture and day. These models showed results consistent with those presented here.

Analysis of explanatory factors

We conducted analyses to examine correlations between evolved strategies and three sets of potential explanatory variables. The first set of analyses considered five location variables that provide a broad biogeographic description of each location: distance to coast, elevation, latitude, mean annual precipitation and mean annual temperature. The second set of analyses focused on six variables that quantify climatic variance and predictability: the mean annual coefficient of variation for daily maximum temperature, the mean annual coefficient of variation for daily precipitation total, the coefficient of variation for annual mean daily maximum temperatures, the coefficient of variation for annual mean daily precipitation totals, the lag=1 autocorrelation coefficient for daily maximum temperature, and the lag=1 autocorrelation coefficient for daily precipitation totals. The first two of these variables provide metrics of intra-annual climatic variation, the second two provide metrics of inter-annual climatic

variation, and the last two provide metrics of short-term predictability. The third set of analyses used six published metrics of climatic predictability, variability and seasonality[12,30]: Lisovski et al.'s predictability and seasonality metrics for temperature and precipitation, and Pau et al.'s variance metrics for temperature and precipitation. Because the Pau et al. and Lisovski et al. metrics of seasonality were highly correlated, we did not also include the Pau et al. metrics of seasonality.

These analyses used a dataset composed of the mean strategies that evolved in each simulation conducted in each location. For each analysis set, we used linear mixed models including all *a priori* explanatory variables as fixed factors for each trait effect dimension, with an additional random factor to allow intercepts to vary by location. We find qualitatively identical results using logit-transformed trait effects, but present analyses of untransformed data here so that the effect sizes are reported in interpretable units (Extended Data Fig. 6).

Climate change scenarios

We examined how the individuals from the final generation of each simulation performed in novel climate regimes using two simple climate change scenarios. In the "shift" scenario, we advanced the historic temperature and precipitation regime in each year by 5 days. In the "warming" scenario, we increased all daily temperatures by 3 degrees; the precipitation regime was unchanged. In both scenarios, we calculated the emergence, fitness, and Aitchison compositional mean [29] of the trait effects that would have been realized for each individual in each unique year of the modified climate regime. This allowed us to assess how climate change affected the phenotype and fitness consequences of each genotype that evolved under historical conditions.

We assessed correlations between each trait effect (T) and the change in emergence timing, and between each trait effect and geometric mean fitness for each evolved genotype, in all cases using linear mixed models with location as a random factor allowing intercepts and slopes to vary.

References

1. Parmesan, C. & Yohe, G. A globally coherent fingerprint of climate change impacts across natural systems. *Nature* **421,** 37–42 (2003).

2. Thackeray, S. J. *et al.* Trophic level asynchrony in rates of phenological change for marine, freshwater and terrestrial environments. *Glob. Change Biol.* **16,** 3304–3313 (2010).

3. Parmesan, C. Influences of species, latitudes and methodologies on estimates of phenological response to global warming. *Glob. Change Biol.* **13,** 1860–1872 (2007).

4. Pearse, W. D., Davis, C. C., Inouye, D. W., Primack, R. B. & Davies, T. J. A statistical estimator for determining the limits of contemporary and historic phenology. *Nat. Ecol. Evol.* **1,** 1876–1882 (2017).

5. Visser, M. E. & Both, C. Shifts in phenology due to global climate change: the need for a yardstick. *Proc. R. Soc. Lond. Ser. B* **272,** 2561–2569 (2005).

6. Both, C., Van Asch, M., Bijlsma, R. G., Van Den Burg, A. B. & Visser, M. E. Climate change and unequal phenological changes across four trophic levels: constraints or adaptations? *J. Anim. Ecol.* **78,** 73–83 (2009).

7. Rafferty, N. E., CaraDonna, P. J. & Bronstein, J. L. Phenological shifts and the fate of mutualisms. *Oikos* **124,** 14–21 (2015).

8. Kharouba, H. M. *et al.* Global shifts in the phenological synchrony of species interactions over recent decades. *Proc. Natl. Acad. Sci.* 201714511 (2018). doi:10.1073/pnas.1714511115

9. Parmesan, C. Ecological and evolutionary responses to recent climate change. *Annu. Rev. Ecol. Evol. Syst.* **37,** 637–669 (2006).

10. Forrest, J. & Miller-Rushing, A. J. Toward a synthetic understanding of the role of phenology in ecology and evolution. *Philos. Trans. R. Soc. B Biol. Sci.* **365,** 3101–3112 (2010).

11. Visser, M. E., Caro, S. P., Oers, K. van, Schaper, S. V. & Helm, B. Phenology, seasonal timing and circannual rhythms: towards a unified framework. *Philos. Trans. R. Soc. B Biol. Sci.* **365,** 3113–3127 (2010).

12. Pau, S. *et al.* Predicting phenology by integrating ecology, evolution and climate science. *Glob. Change Biol.* **17,** 3633–3643 (2011).

13. Chmura, H. *et al.* The mechanisms of phenology: the patterns and processes of phenological shifts. *Ecol. Monogr.* (in press).

14. Molina-Montenegro, M. A. & Naya, D. E. Latitudinal patterns in phenotypic plasticity and fitness-related traits: assessing the climatic variability hypothesis (CVH) with an invasive plant species. *PLOS ONE* **7,** e47620 (2012).

15. Sunday, J. M., Bates, A. E. & Dulvy, N. K. Global analysis of thermal tolerance and latitude in ectotherms. *Proc. R. Soc. B-Biol. Sci.* **278,** 1823–1830 (2011).

16. Grishkevich, V. & Yanai, I. The genomic determinants of genotype × environment interactions in gene expression. *Trends Genet.* **29,** 479–487 (2013).

17. Thackeray, S. J. *et al.* Phenological sensitivity to climate across taxa and trophic levels. *Nature* **535,** 241–245 (2016).

18. McGuigan, K., Nishimura, N., Currey, M., Hurwit, D. & Cresko, W. A. Cryptic Genetic Variation and Body Size Evolution in Threespine Stickleback. *Evolution* **65,** 1203–1211 (2011).

19. Ghalambor, C. K., McKay, J. K., Carroll, S. P. & Reznick, D. N. Adaptive versus non-adaptive phenotypic plasticity and the potential for contemporary adaptation in new environments. *Funct. Ecol.* **21,** 394–407 (2007).

20. Coppack, T. & Pulido, F. Photoperiodic Response and the Adaptability of Avian Life Cycles to Environmental Change. in *Advances in Ecological Research* **35,** 131–150 (Academic Press, 2004).

21. Way, D. A. & Montgomery, R. A. Photoperiod constraints on tree phenology, performance and migration in a warming world. *Plant Cell Environ.* **38,** 1725–1736 (2015).

22. Chevin, L.-M. & Lande, R. Evolution of environmental cues for phenotypic plasticity. *Evolution* **69,** 2767–2775 (2015).

23. McNamara, J. M., Barta, Z., Klaassen, M. & Bauer, S. Cues and the optimal timing of activities under environmental changes. *Ecol. Lett.* **14,** 1183–1190 (2011).

24. Climate Data Online (CDO) - The National Climatic Data Center's (NCDC) Climate Data Online (CDO) provides free access to NCDC's archive of historical weather and climate data in addition to station history information. | National Climatic Data Center (NCDC). Available at: https://www.ncdc.noaa.gov/cdo-web/. (Accessed: 7th September 2018)

25. Hau, M., Wikelski, M. & Wingfield, J. C. A neotropical forest bird can measure the slight changes in tropical photoperiod. *Proc. R. Soc. B Biol. Sci.* **265,** 89–95 (1998).

26. Dawson, A. Seasonality in a temperate zone bird can be entrained by near equatorial photoperiods. *Proc. R. Soc. Lond. B Biol. Sci.* **274,** 721–725 (2007).

27. Sinclair, B. J. *et al.* Can we predict ectotherm responses to climate change using thermal performance curves and body temperatures? *Ecol. Lett.* **19,** 1372–1385 (2016).

28. Huey, R. B. & Stevenson, R. D. Integrating Thermal Physiology and Ecology of Ectotherms: A Discussion of Approaches. *Am. Zool.* **19,** 357–366 (1979).

29. Boogaart, K. G. van den & Tolosana-Delgado, R. *Analyzing Compositional Data with R*. (Springer Science & Business Media, 2013).

30. Lisovski, S., Ramenofsky, M. & Wingfield, J. C. Defining the degree of seasonality and its significance for future research. *Integr. Comp. Biol.* icx040–icx040 (2017). doi:10.1093/icb/icx040

Acknowledgements

We thank Stephen Ellner, Andy Sih, Sebastian Schreiber, Jay Rosenheim, and Jaime Ashander for comments on the development of this work. CBE was supported by an NSF Graduate Research Fellowship, and LHY was supported by NSF DEB-1253101.

Author Contributions

Both authors contributed equally to this work.

Author Information

We do not have any competing financial and/or non-financial interests in relation to the work described.

Correspondence and requests for materials should be addressed to lhyang@ucdavis.edu and cbe36@cornell.edu

Figures

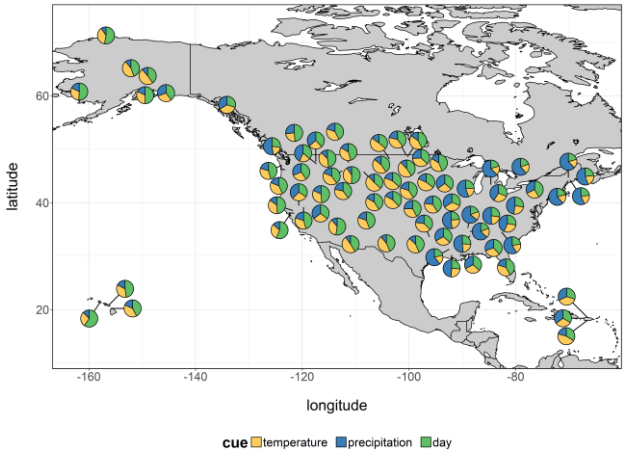

Figure 1. Evolved strategies show spatial autocorrelation in relative cue use (T); similar strategies evolve in nearby locations with similar climates, and different strategies evolves in distant locations with different climates.

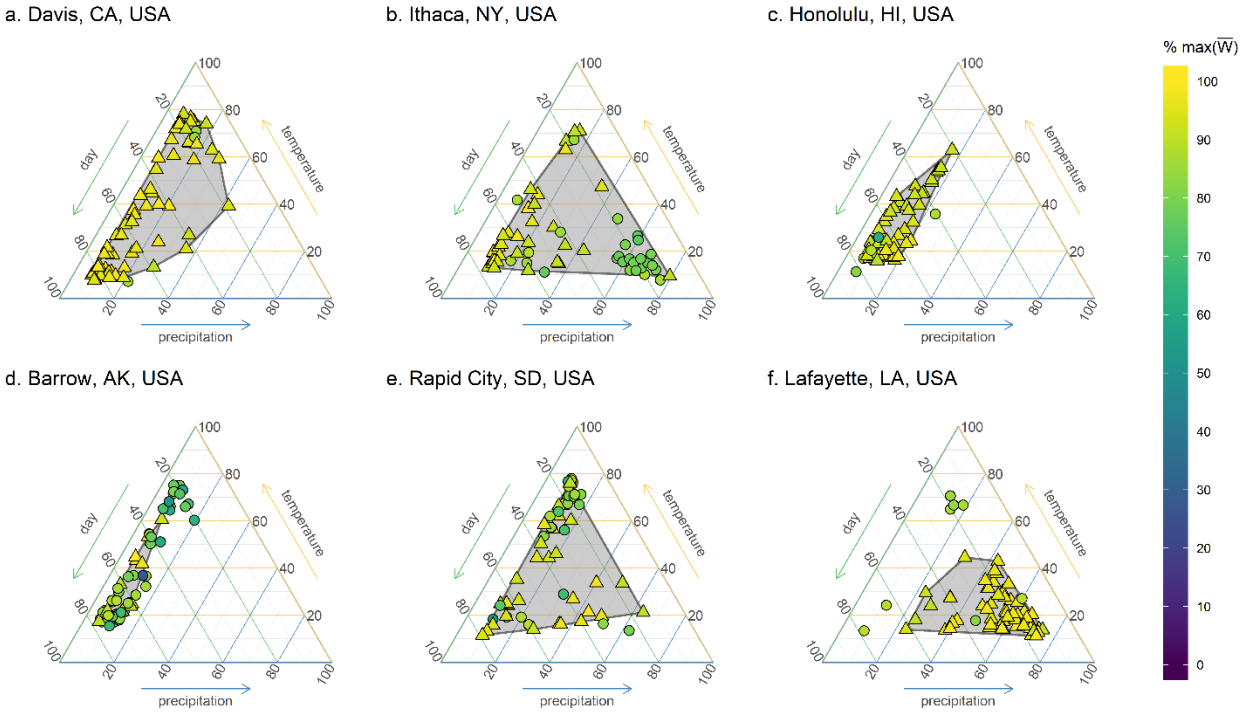

Figure 2. Ternary plots illustrate proportional cue use at the time of emergence for six selected locations. Each point represents the mean strategy at the end of one simulation; each strategy is represented as a composition of the trait effects (T) in percents, which represent relative cue use (see "assessing realized relative cue use" in Methods). Point color reflects geometric mean fitness as a percent of the maximum geometric mean fitness ($\overline{W}$) for each location. Simulations within 10% of the maximum observed geometric mean fitness in each location are represented as triangles and included in a gray convex hull. All other points are represented as circles. Ternary plots for all 78 locations are presented in Extended Data Fig. 1, locations are described in Extended Data Table 1.

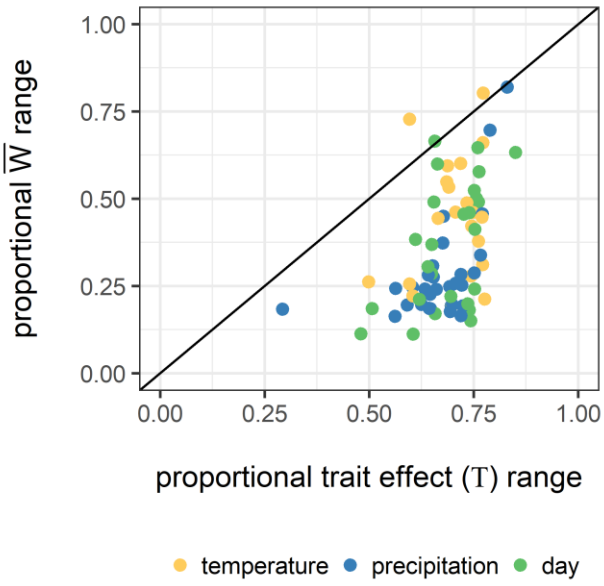

Figure 3. Cryptic genetic variation persists under selection in part because a wide range of genotypes show similar phenotypes and fitness outcomes. Each point represents the maximum proportional range of trait effects (T) and the maximum proportional range of geometric mean fitness ($\overline{W}$) of final populations across 30 simulations for each of 78 locations. The null expectation is shown as a solid line. Strategies show a wide range trait effects with relatively small effects on mean geometric fitness. The color of each point depicts which of the three trait effects produced the maximum proportional range depicted.

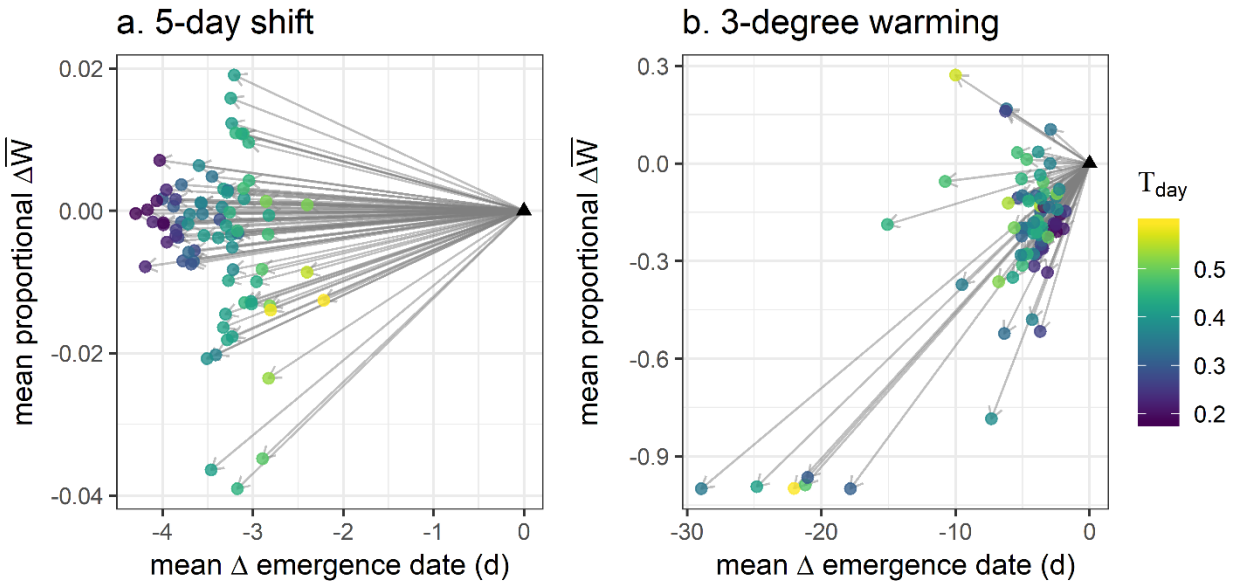

Figure 4. Under two climate change scenarios, organisms with different environmental histories generally emerge earlier, but show variable degrees of advancement and highly variable fitness consequences. The position of each circle represents the mean change in emergence day and the proportional change in geometric mean fitness averaged across all evolved genotypes of 60 simulations for each of 78 locations, relative to the historical climate in that location, represented by a black triangle. The color of each circle represents the historical trait effect of day (T_{day}), indicating the relative use of a climatically invariant cue.

Supplementary Information

Supplementary Videos 1-6. Animated 3-D view of fitness surfaces

Supplementary Table 1. Location data

Extended Data

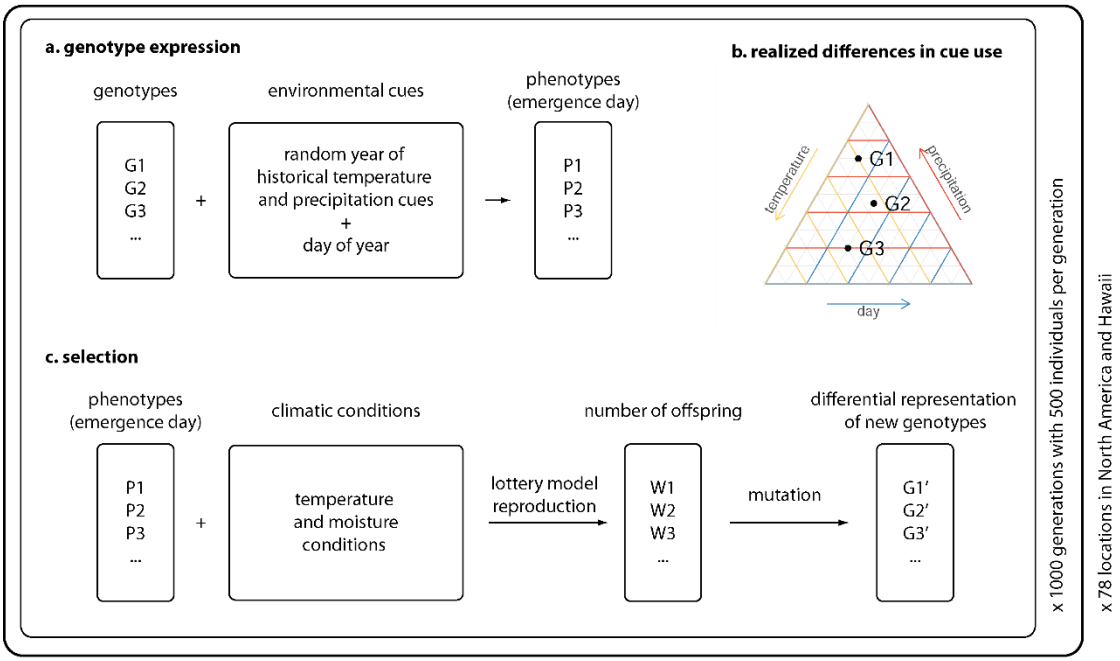

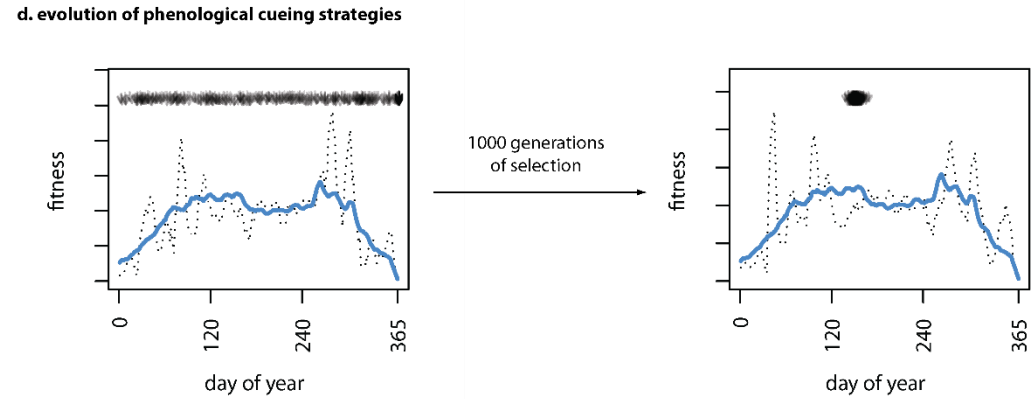

Figure 1. Schematic diagram of model. a.) Genotypes combined with environmental cues (including cumulative annual daily temperature maximums, cumulative annual daily precipitation totals and day of year) result in expressed phenotypes (emergence days). b.) The proportional contribution of each trait to the first emergence decision (a representation of the interaction between genotype and environment) can be expressed as a composition and presented on a ternary plot. c.) The fitness of different phenotypes is determined by climatic (temperature and moisture) conditions during a 10-day window after emergence. A lottery model of reproduction determines the number of offspring produced by each individual, and mutation results in new genotypes for the next generation. d.) Selection results in evolved phenological cueing strategies that anticipate favorable conditions and avoid unfavorable conditions. In this panel, the solid blue line represents the long-term expected fitness outcome for each day under historical conditions, while the dotted black lines represent the fitness outcomes for the first and last year of the simulation for the left and right panels respectively. The black arrows at the top of each panel represent the emergence timing of the population. Initially emergence is

spread across the year, but after 1000 generations of selection, most of the population shows similar emergence timing.

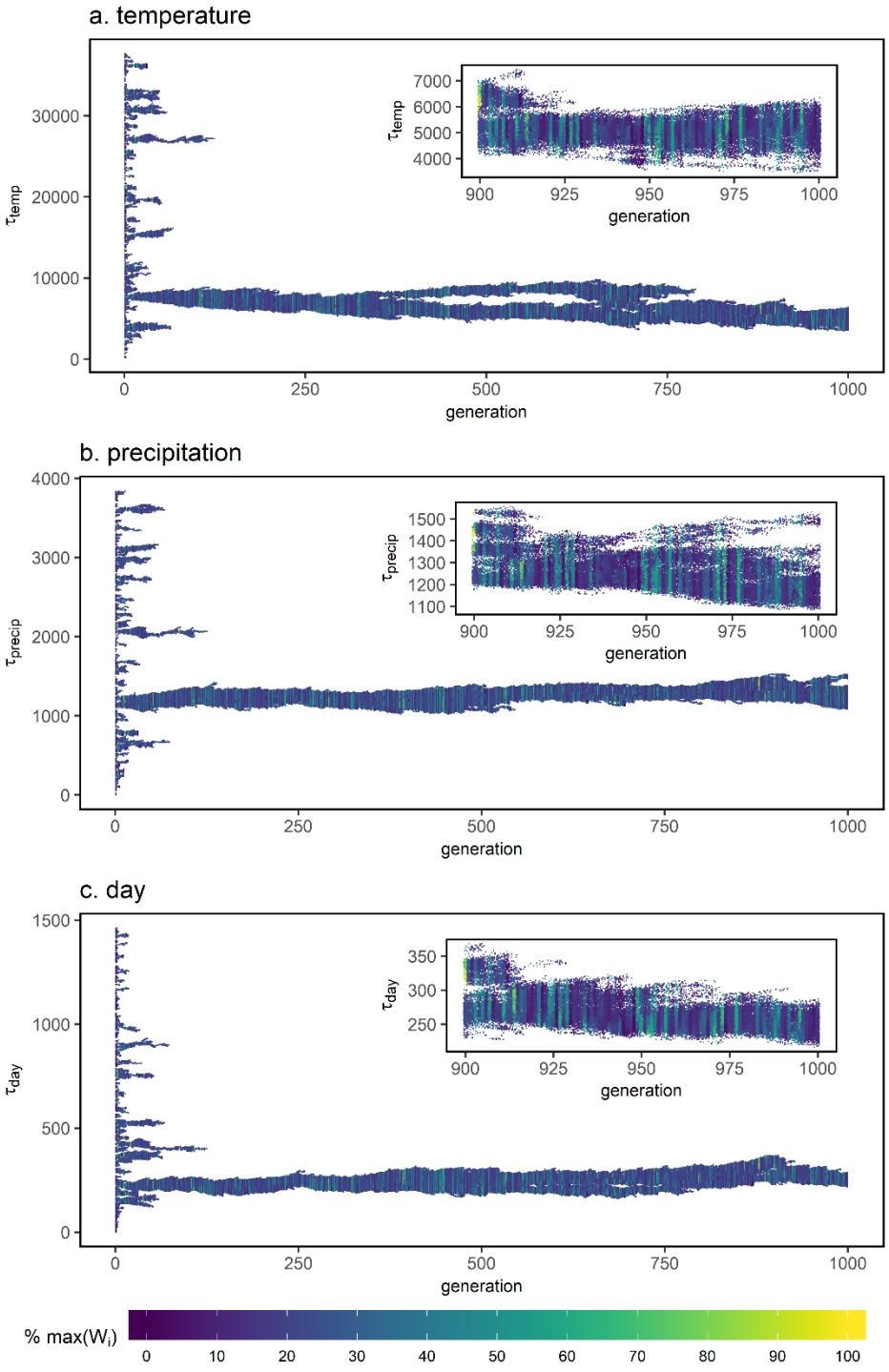

Figure 2. Temperature, precipitation and day traits evolve over 1000 generations in this representative simulation from Davis, CA. Each simulation begins with a broad uniform distribution of initial values for each trait; selection drives the evolution of specific strategies. The inset figure shows an expanded view

of trait evolution in the final 100 generations. Each point represents the trait value of one individual; point colors show individual fitness proportional to the maximum value in this simulation.

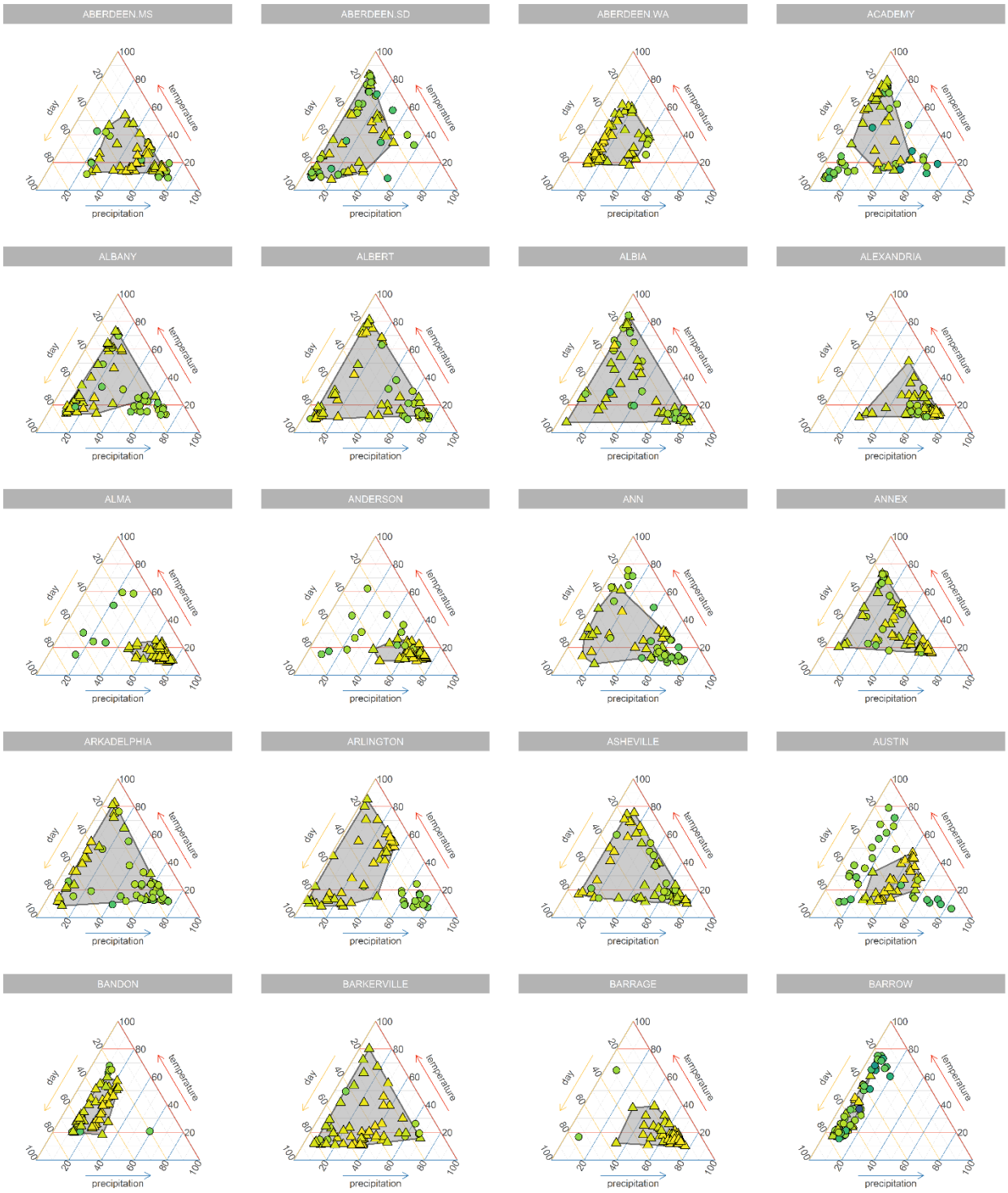

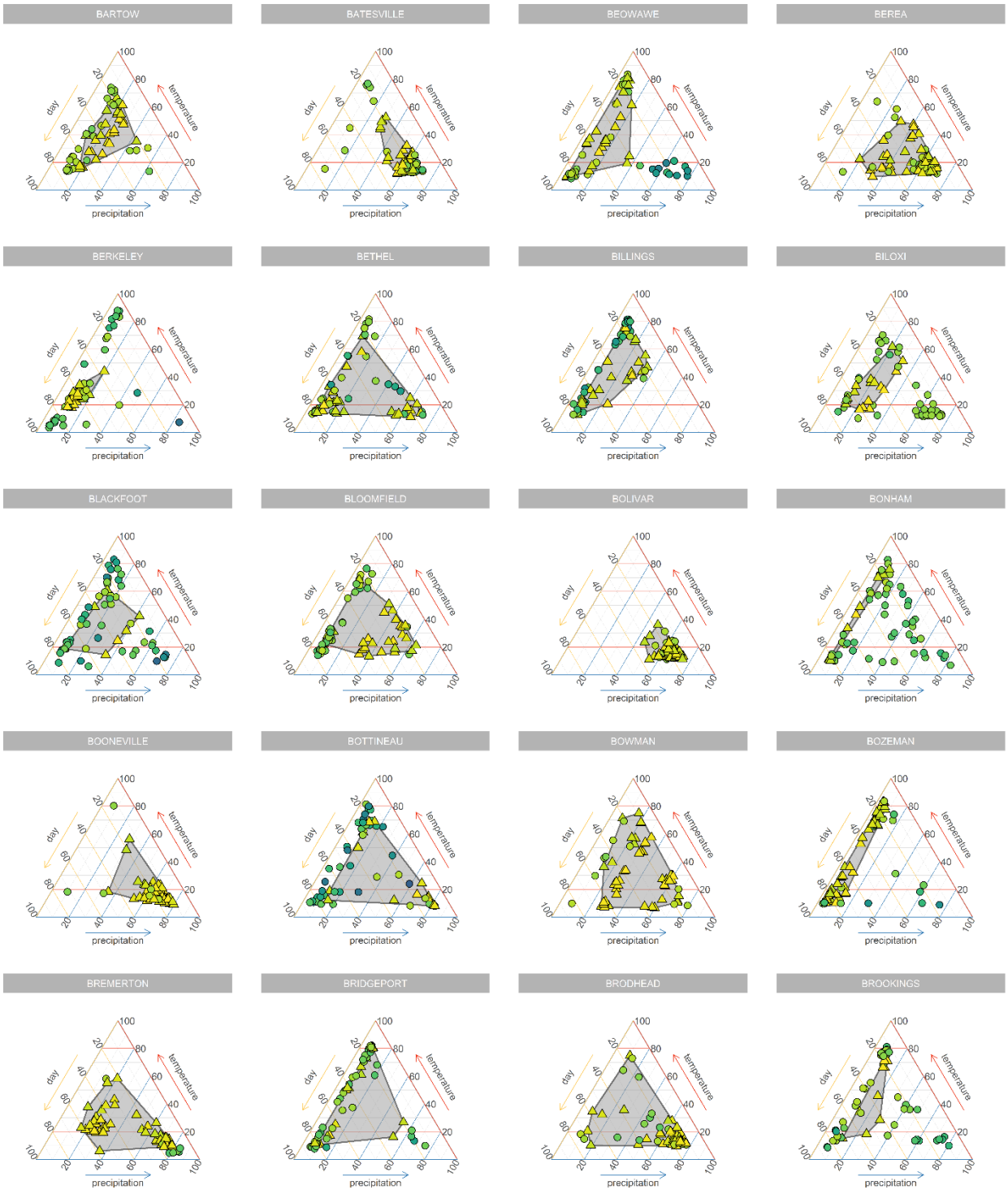

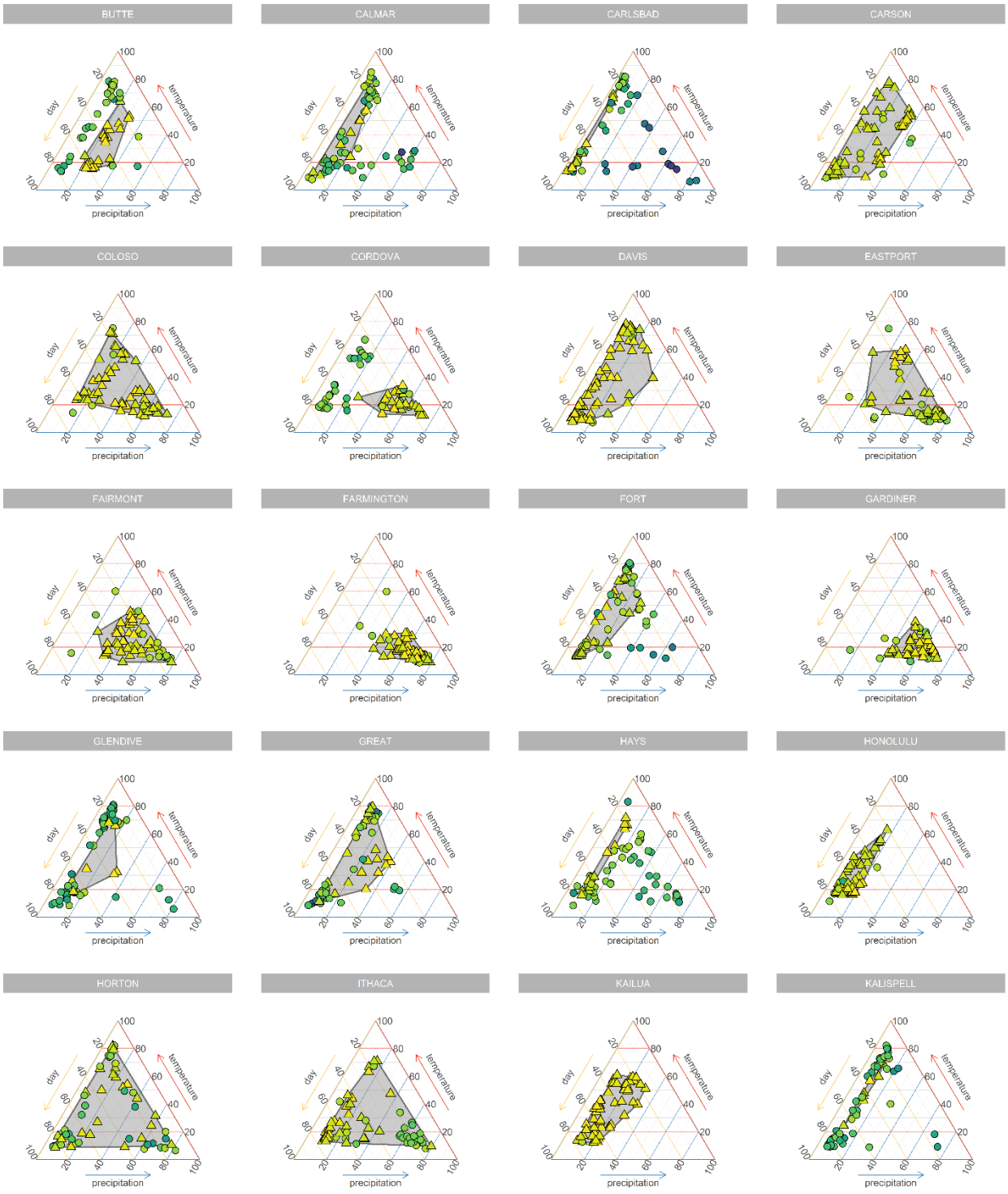

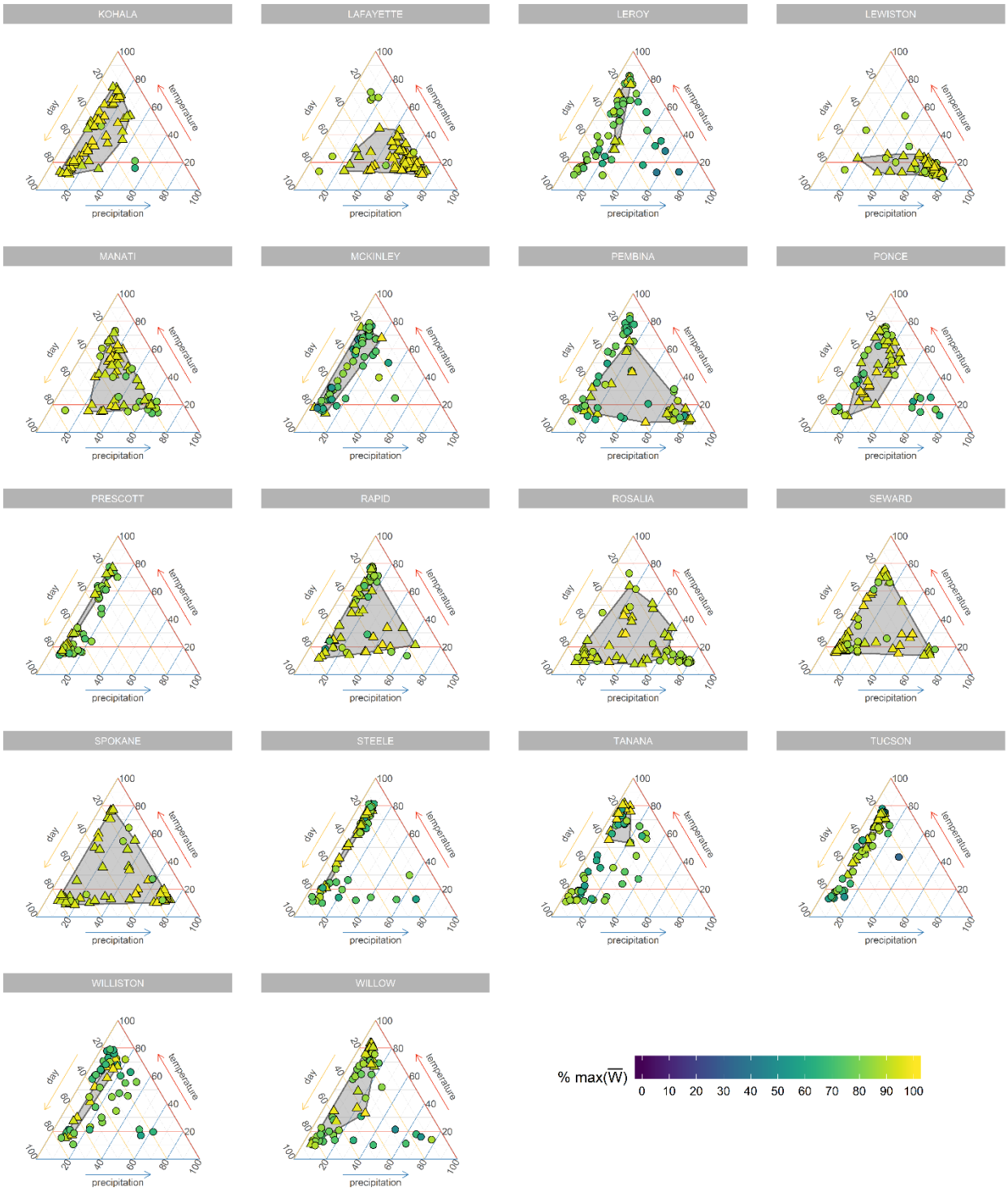

Figure 3. Evolved strategies for 30 simulations in each of 78 locations. Each point represents the mean strategy at the end of one simulation; each strategy is represented as a composition of the "trait effects" in percents, which represent relative cue use (see "assessing realized relative cue use" in Methods). Point color reflects the mean geometric mean fitness for each simulation scaled by location. Simulations within 10% of the maximum observed geometric mean fitness in each location are represented as triangles and included in a gray convex hull. All other points are represented as circles.

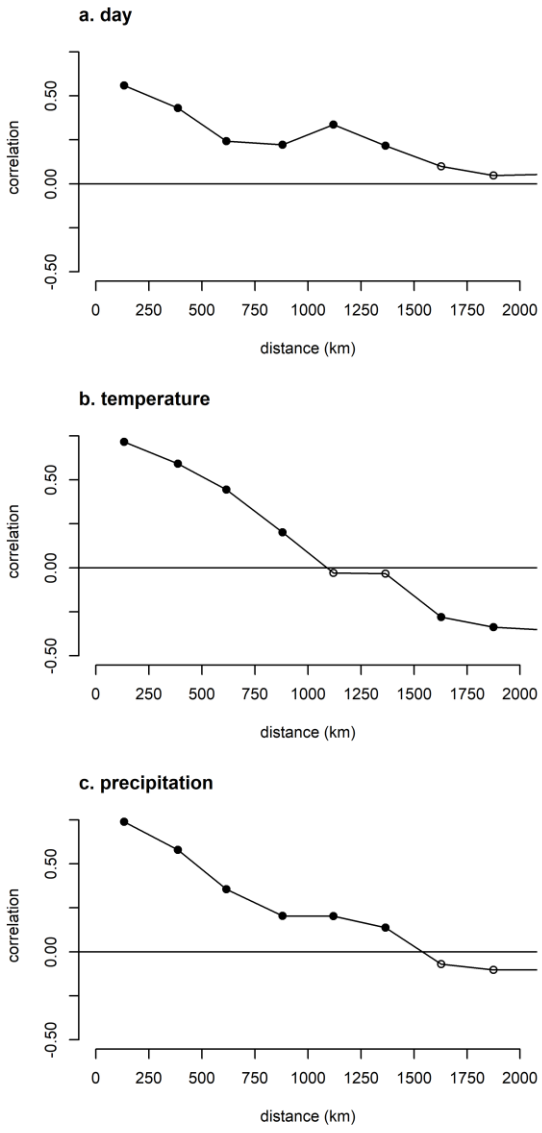

Figure 4. Spatial autocorrelation in reliance on day, temperature and photoperiod cues. Evolved strategies show significant positive spatial autocorrelation in reliance on a) day, b) temperature, and c) precipitation cues up to at least 1000 km. Filled circles are significantly correlated, open circles are not (Moran's I).

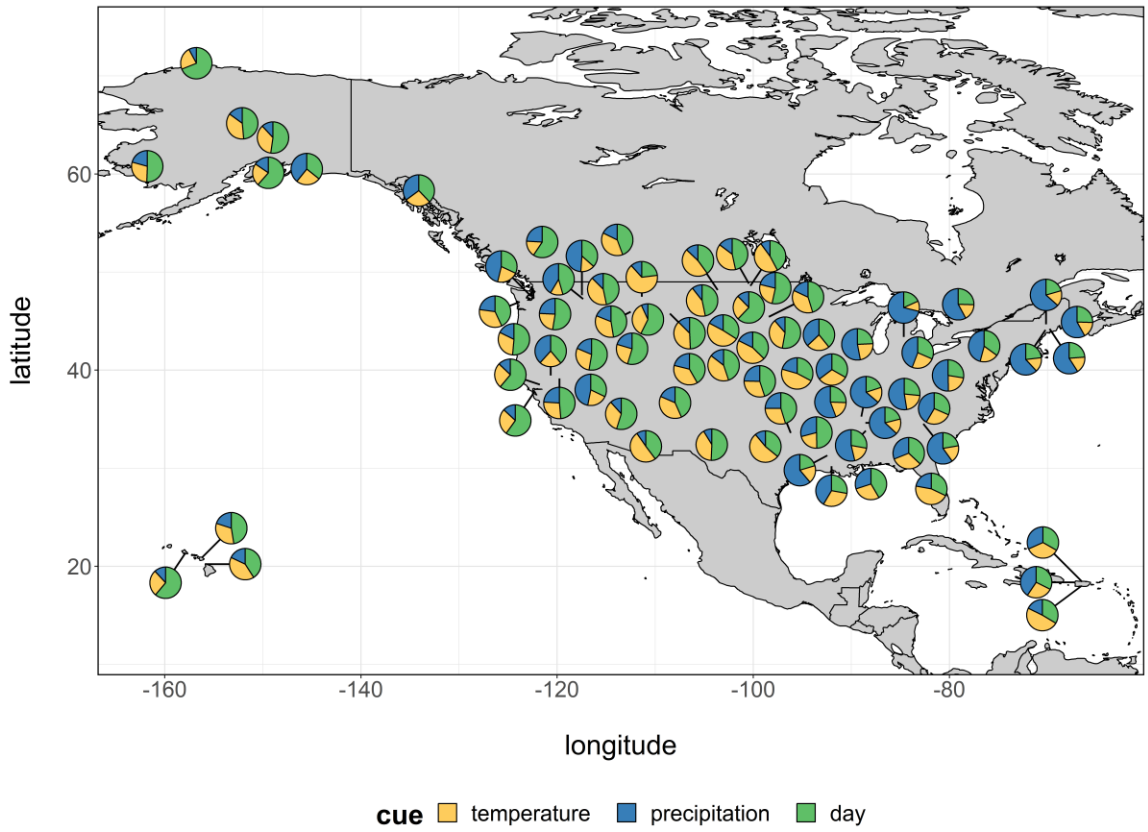

Figure 5. Spatial autocorrelation evolves among phenological cueing strategies in different locations under an alternative model formulation. To generate this alternative map, our model used cumulative photoperiod as the cue for day of year, and we imposed a developmental baseline temperature of 0 C across all locations below which organisms are insensitive to thermal cues.

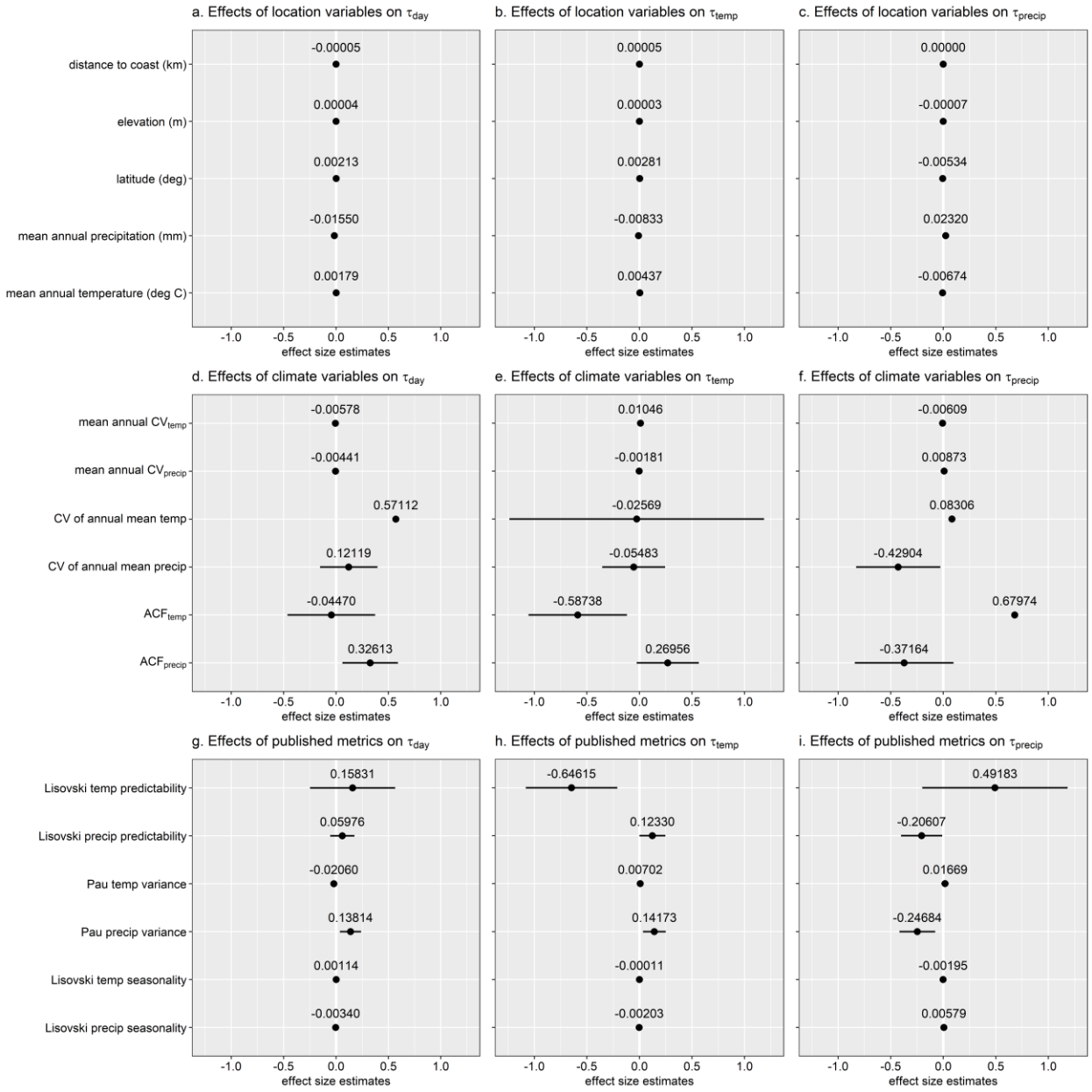

Figure 6. Simple hypothesized explanatory variables were not strongly correlated with evolved strategies. Values indicate fixed effect estimates from linear models (see “Analysis of explanatory factors”).

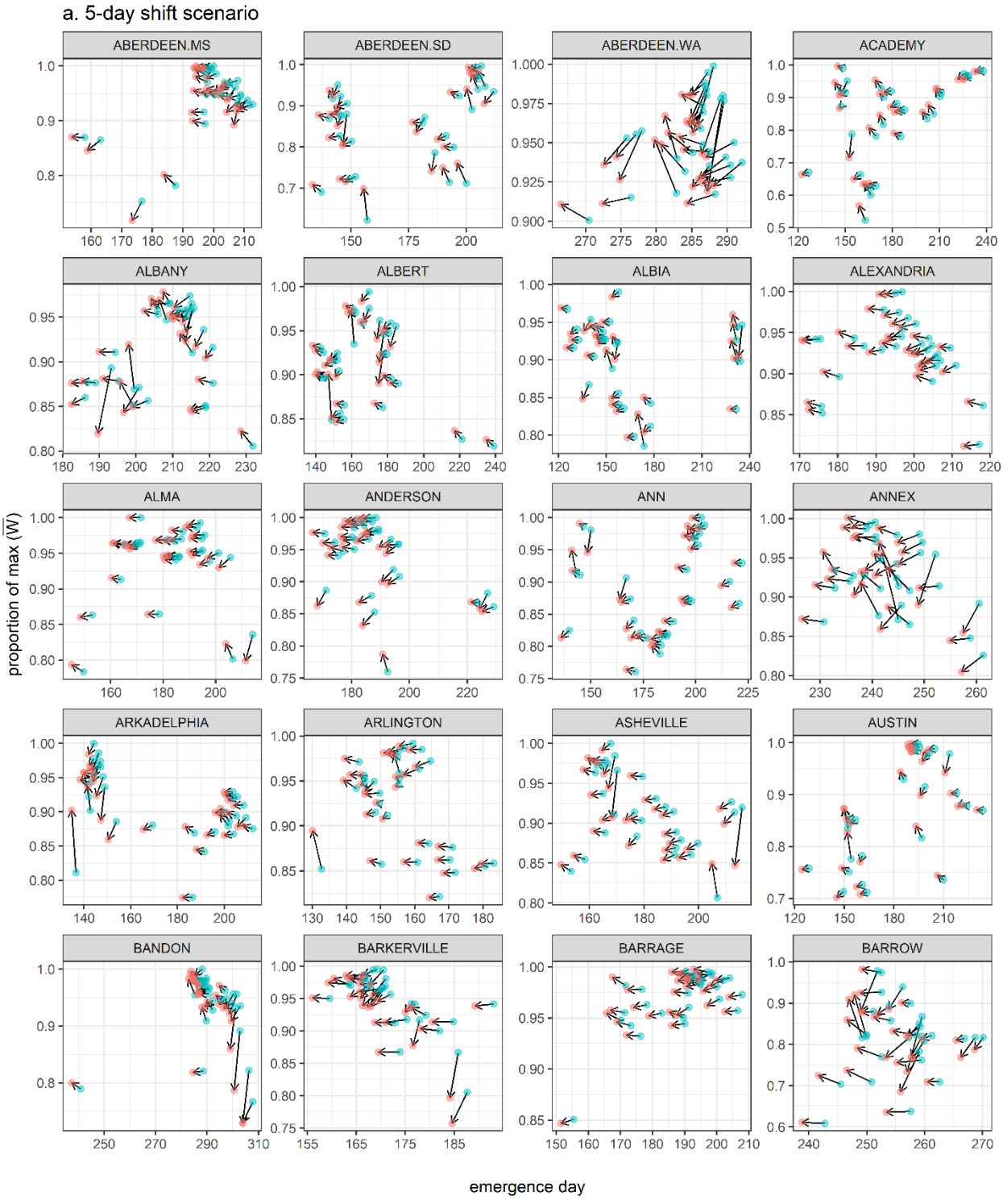

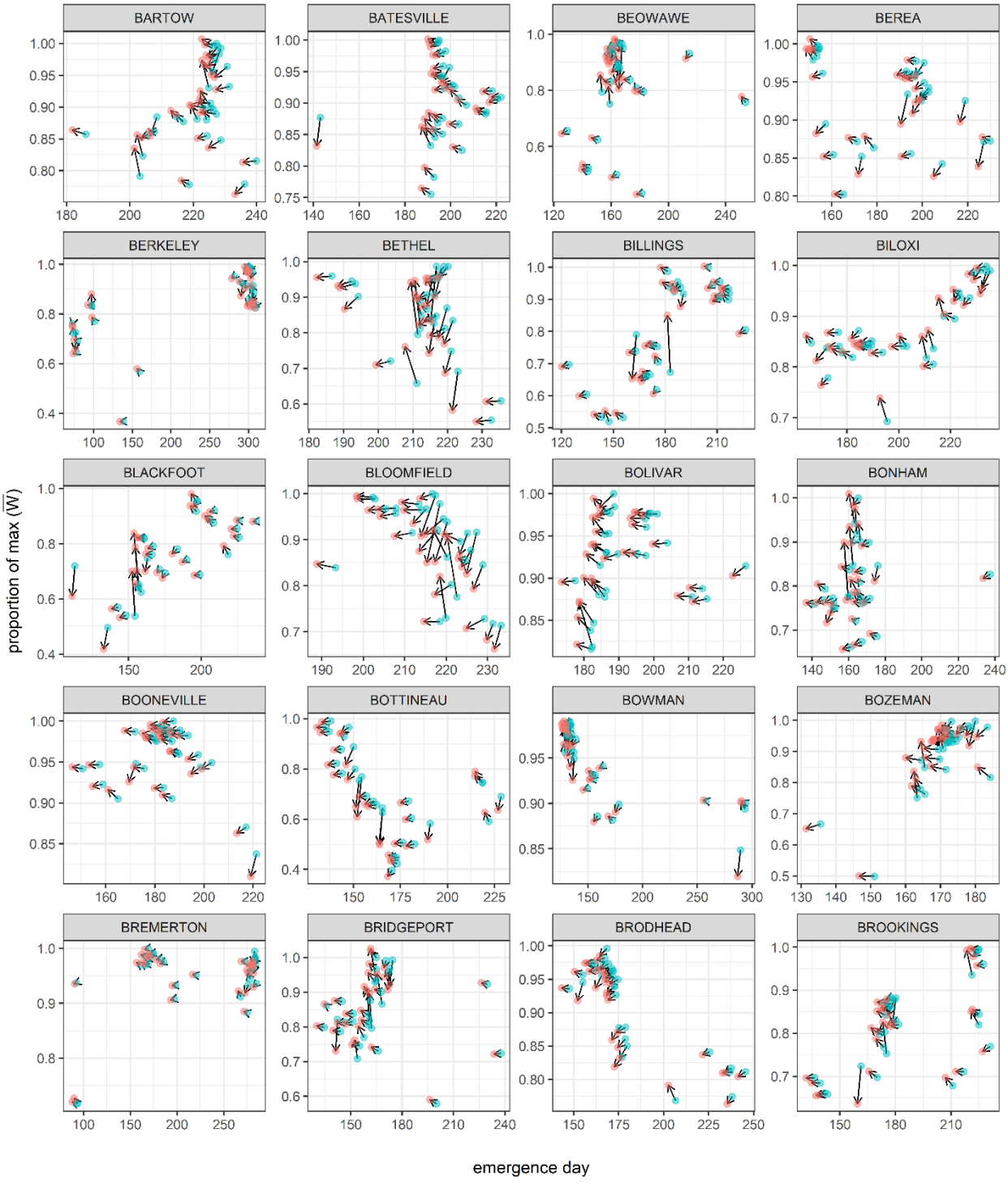

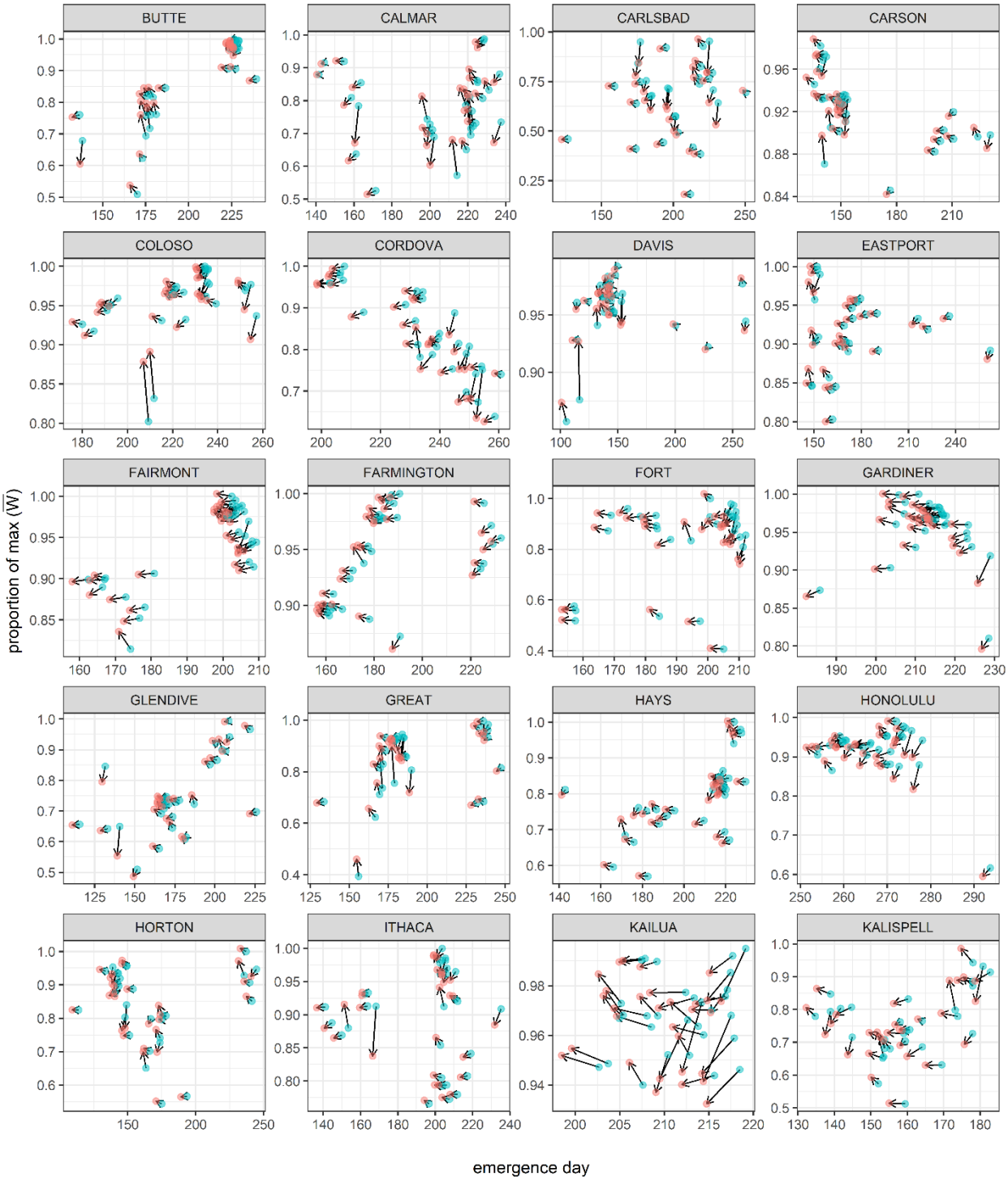

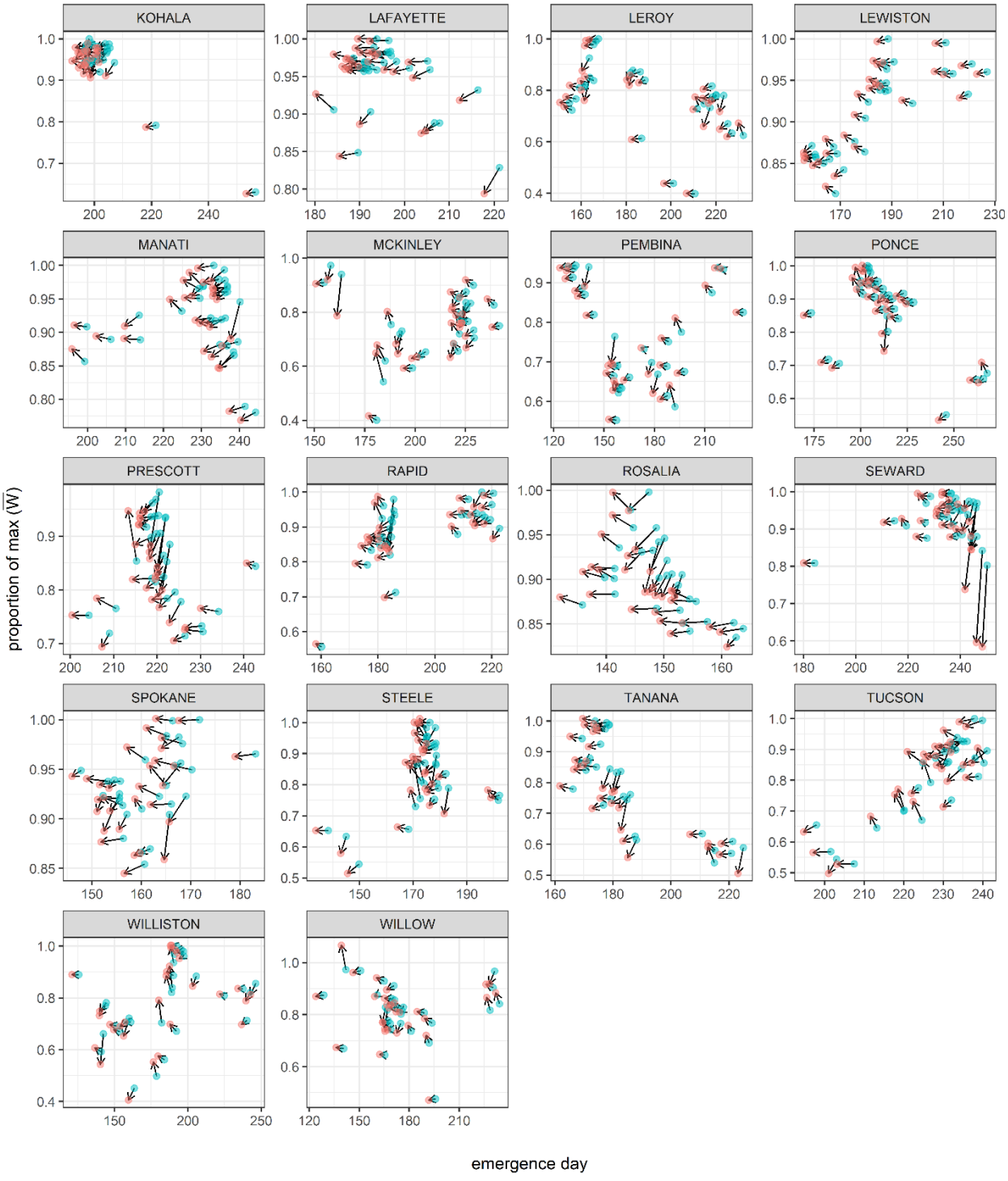

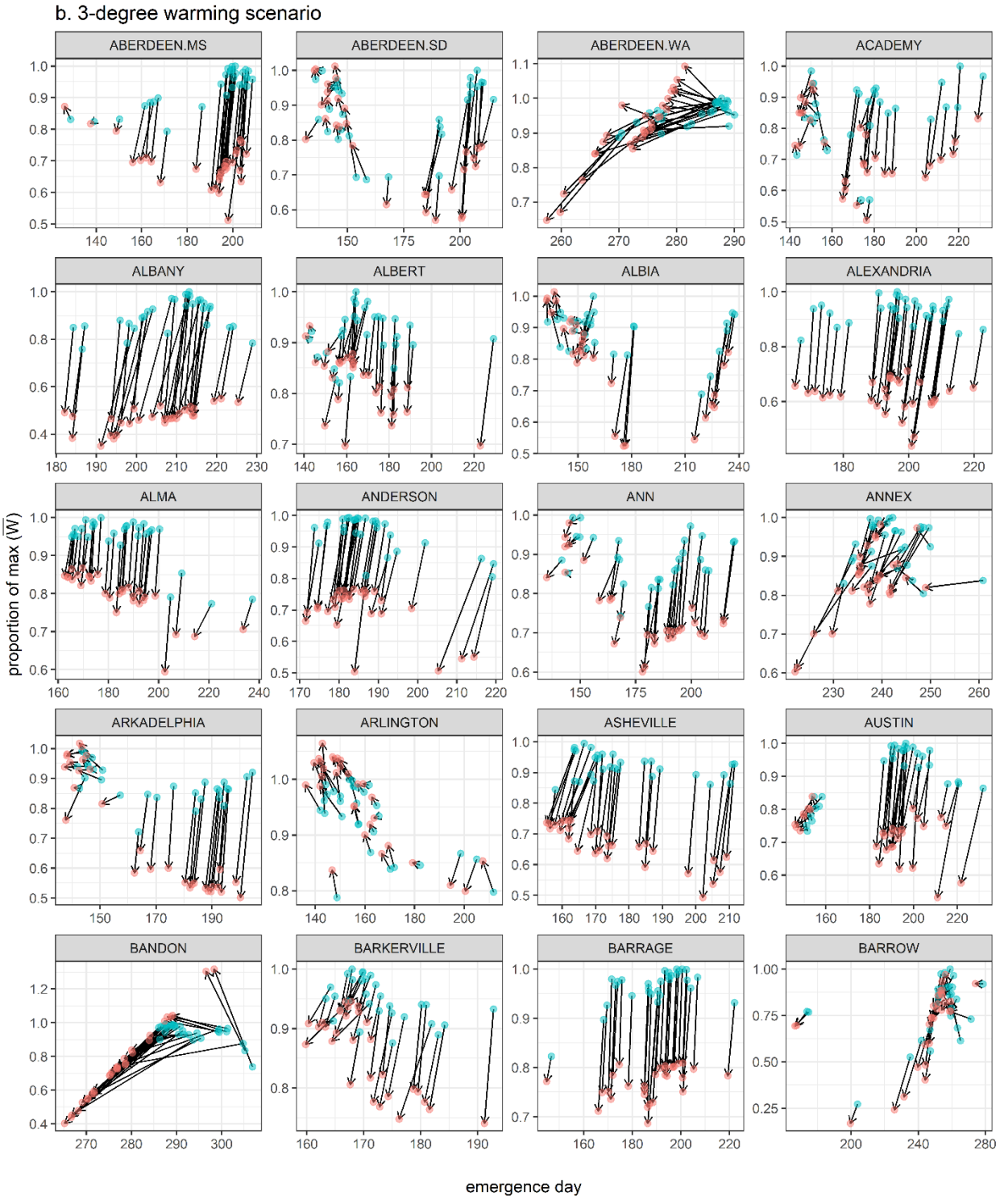

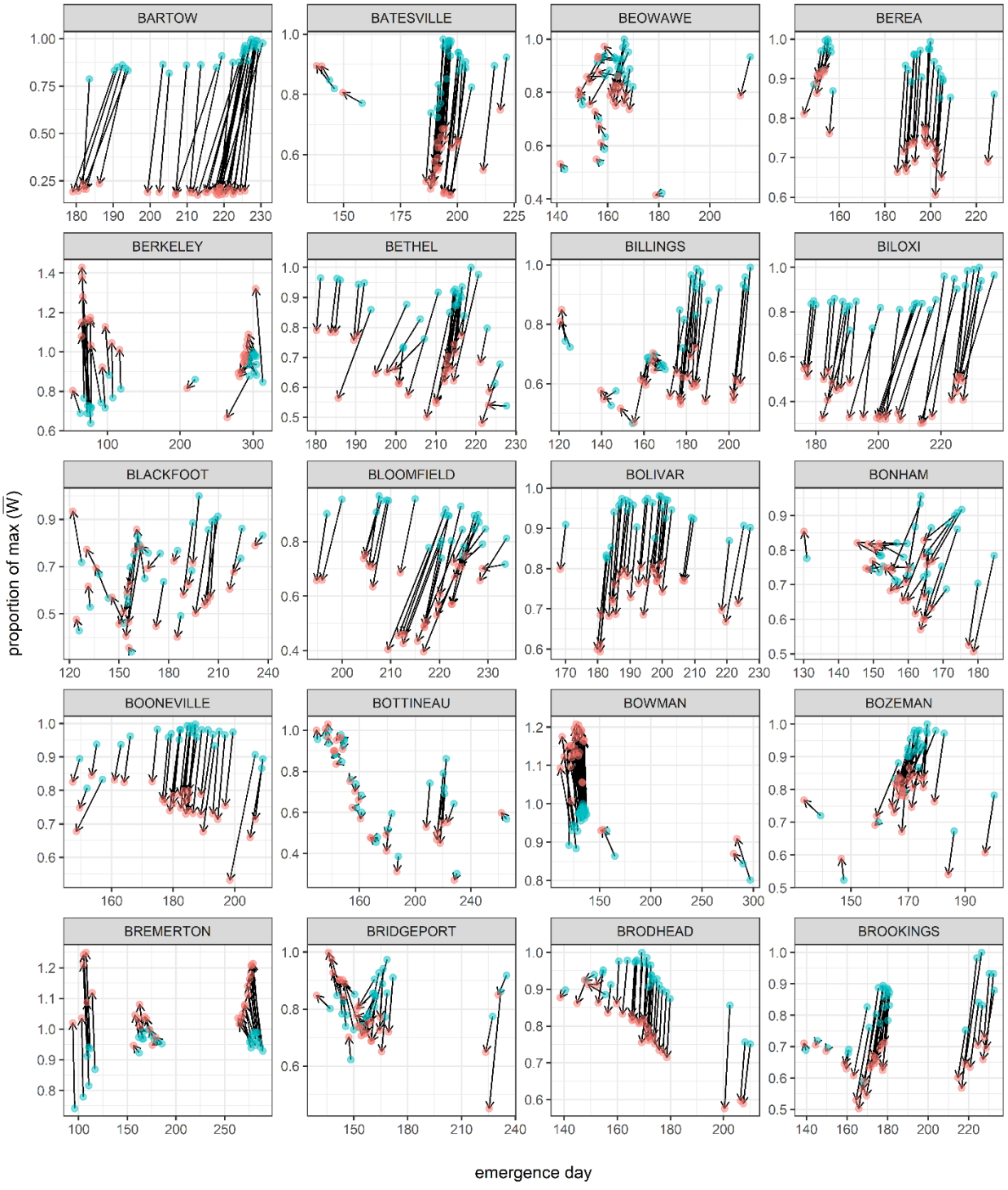

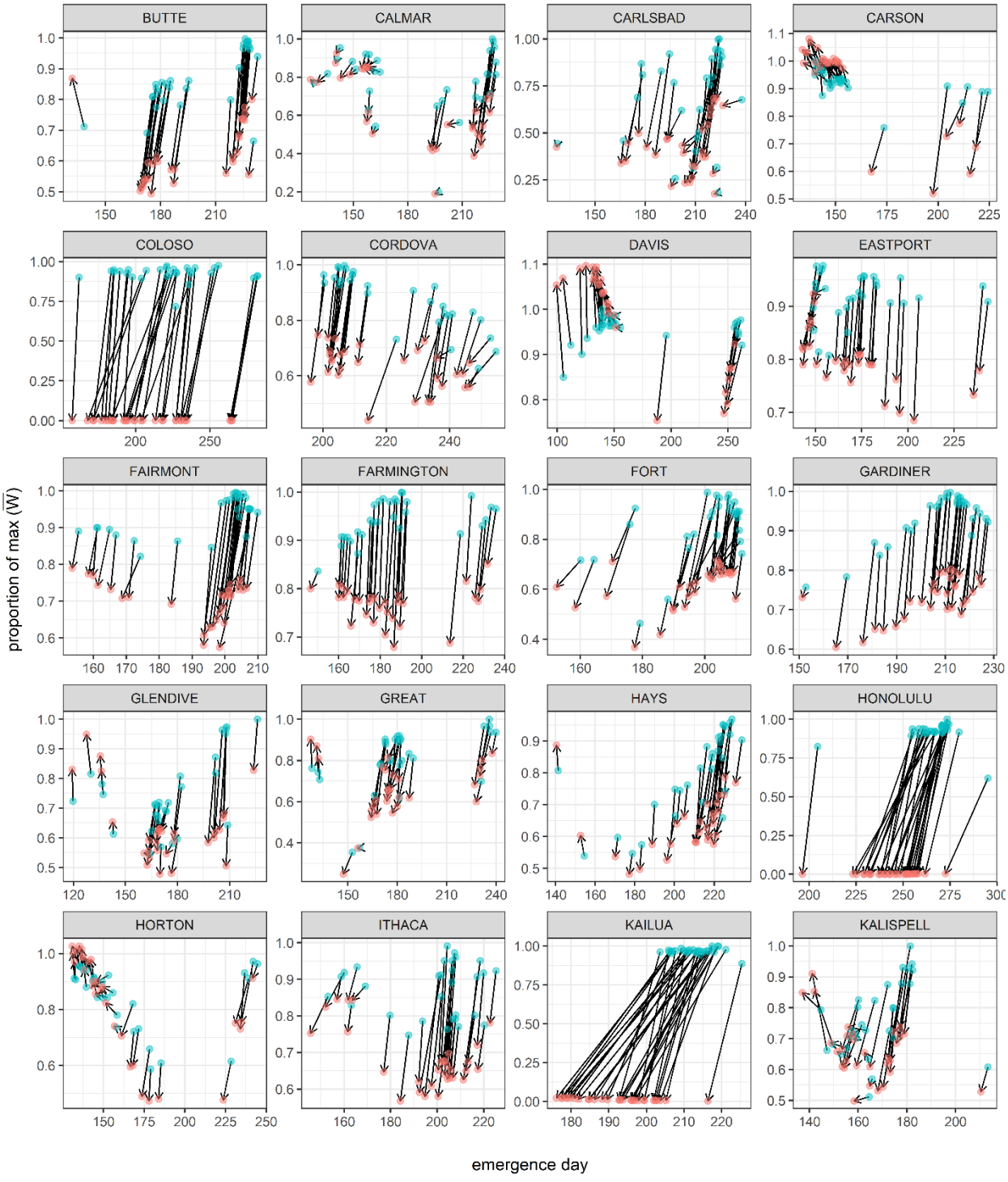

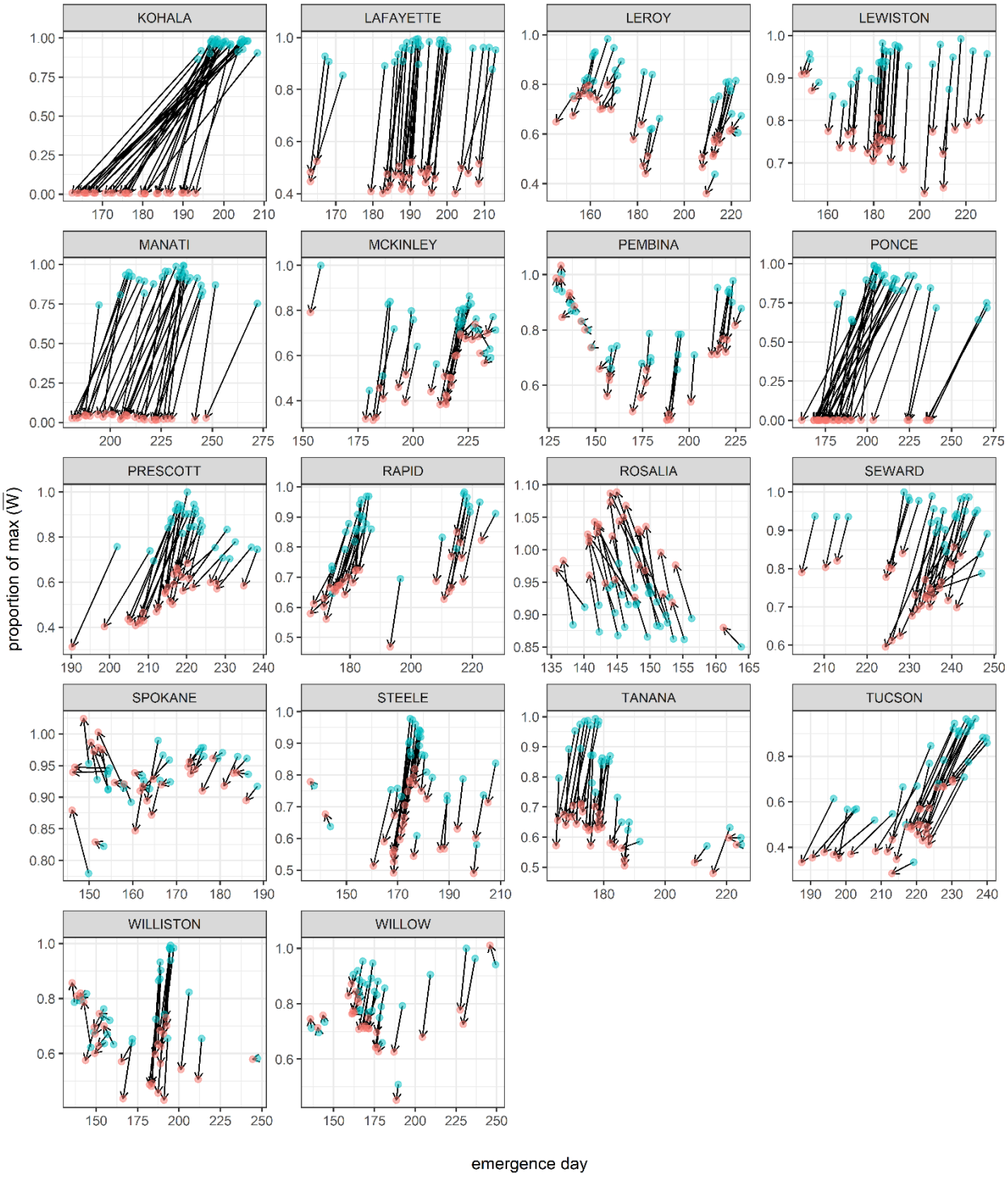

Figure 7. Location specific responses to a) a 5-day shift in temperature and precipitation regimes and b) 3-degree C warming. For each location, each of 30 genotypes is represented by a blue and red circle showing its emergence day and proportional fitness under historical and changed conditions, respectively.

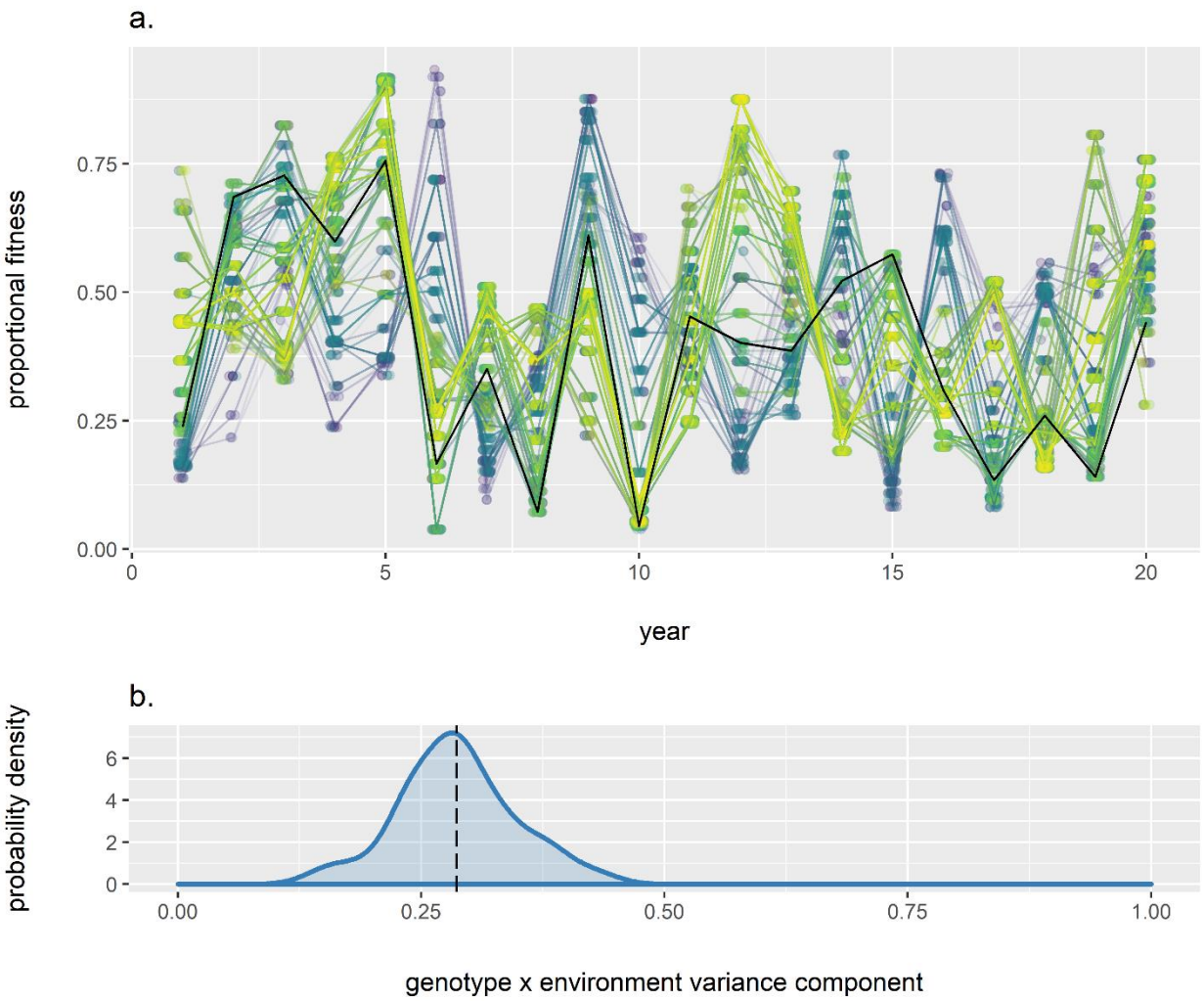

Figure 8. Genotype x environment interactions mean that different genotypes have greater relative fitness advantages in different years; phenological cueing strategies interact with climatic variation to reduce consistent fitness advantages. a.) In this example, each color represents an individual genotype, evaluated in a random subset of 20 years. To facilitate interpretation, a random individual is highlighted as a black line. b.) Genotype x environment interactions account for 29% of fitness variation across all locations on average. The blue probability density function represents the distribution of mean fitness variance components due to genotype x environment interactions in each of 78 locations. The dashed line shows the mean proportion of variation attributable to genotype x environment interactions.

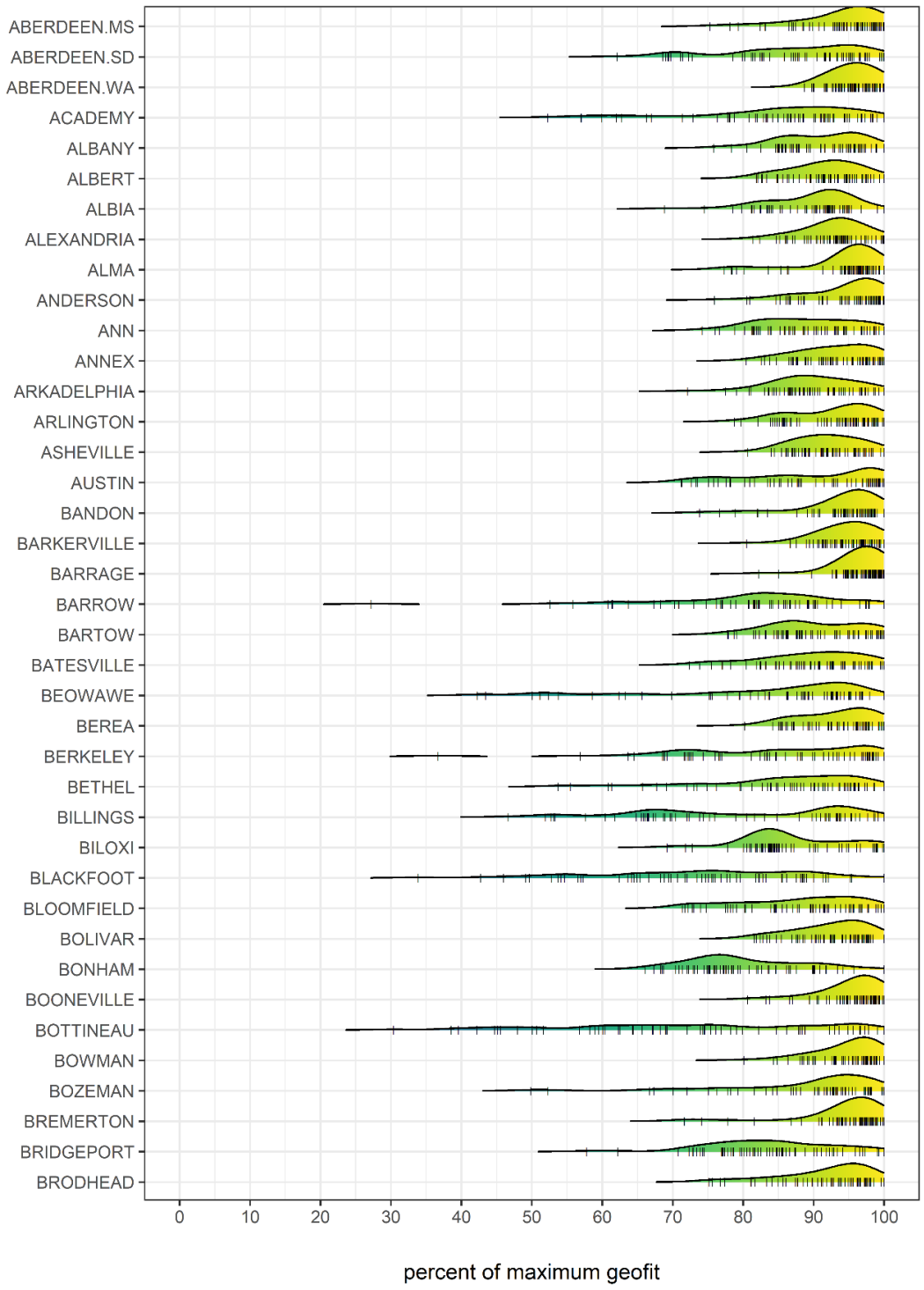

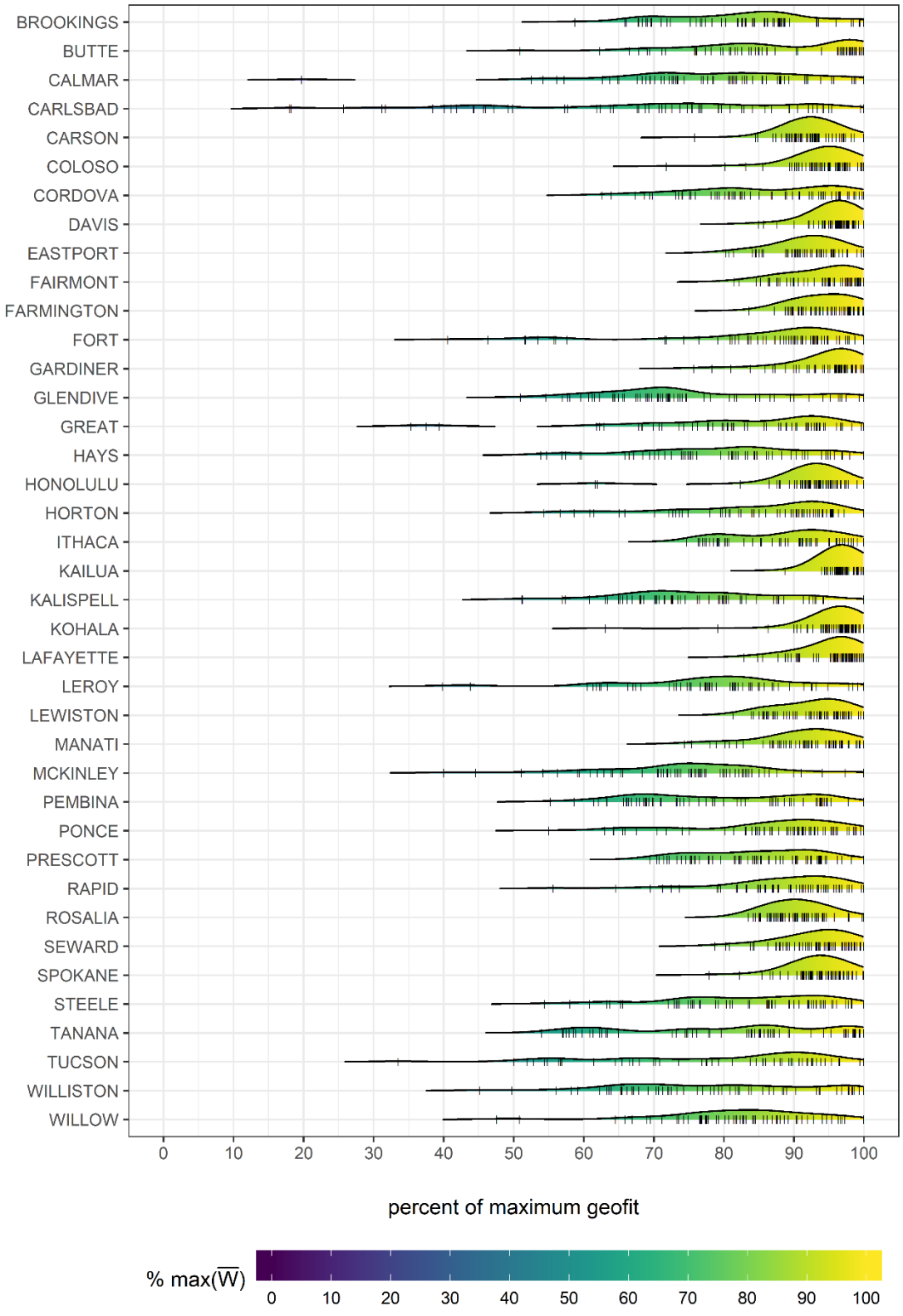

Figure 9. Most simulations result in evolved strategies that have geometric mean fitnesses that are within 10% of the most fit simulation in each location.

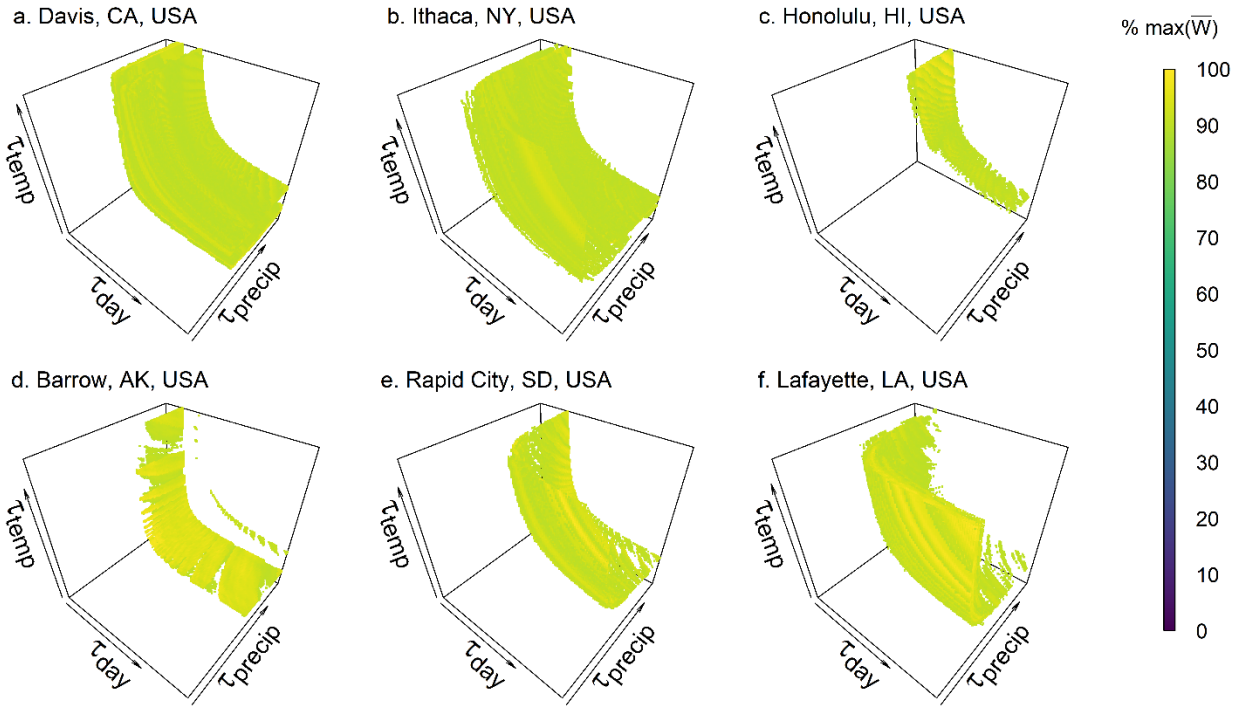

Figure 10. Fitness surfaces. Diverse genotypes can produce similarly high fitness phenotypes. A 100x100x100 grid spanning trait values ranging from the 10th through 90th percentiles of observed cues in each location were evaluated for fitness in each recorded year of climate. Points represent genotypes with geometric mean fitness within 90% of highest observed value in each location, with axes showing the full range of tested points. Animated rotating versions of each panel which better illustrate the three-dimensional structure can be found in Supplementary Videos 1-6.